Towards a method for detecting the potential genotoxicity of nanomaterials

NANOGENOTOX

Deliverable 4.7: Hydrochemical reactivity, solubility, and biodurability of NANOGENOTOX nanomaterials

Key intrinsic physicochemical characteristics of
NANOGENOTOX nanomaterials

March
2013

NANOGENOTOX

Co-funded by
the Health Programme
of the European Union

Grant Agreement n° 2009 21 01

WP 4: Physicochemical Characterization of Manufactured Nanomaterials (MNs) and Exposure Media (EMs)

Deliverable 4.7: Hydrochemical reactivity, solubility, and biodurability of NANOGENOTOX nanomaterials

_

Key intrinsic physicochemical characteristics of NANOGENOTOX nanomaterials

Deliverable leader: NRCWE

Keld Alstrup Jensen
The National Research Centre for the Working Environment (NRCWE),
Lersø Parkallé 105, DK-2100 Copenhagen, DENMARK

National Research Centre
for the Working Environment

Workflow	
Author(s)	**Reviewer(s)**
Keld Alstrup Jensen, Yahia Kembouche, and Signe H. Nielsen (NRCWE)	WP Leader: Keld Alstrup Jensen (NRCWE) Coordinator: Nathalie Thieriet (ANSES)

Document status: v.1   final revision and review by KAJ
Creation date: 18/03/2013

Confidentiality level of the deliverable		
PU	Public	PU
CO	Confidential, only for members of the consortium (including the Commission Services)	

Co-funded by
the Health Programme
of the European Union

1   Introduction

This report is the last of the seven deliverable 4 final reports on the primary and physico-chemical characterization of the MN used in the EAHC-funded NANOGENOTOX Joint action. The complete list of final physico-chemical characterization reports include:

> D4.1: Summary report on primary physiochemical properties of manufactured nanomaterials used in NANOGENOTOX
>
> D4.2: Transmission electron characterization of NANOGENOTOX nanomaterials and comparison with and atomic force microscopy
>
> D4.3: Crystallite size, mineralogical and chemical purity of NANOGENOTOX nanomaterials
>
> D4.4: Determination of specific surface area of NANOGENOTOX nanomaterials
>
> D4.5: Surface charge, hydrodynamic size and size distributions by zetametry, dynamic light scattering (DLS) and small-angle X-ray scattering (SAXS) in optimum aqueous suspensions for titanium and silicon dioxide
>
> D4.6: Dustiness of NANOGENOTOX nanomaterials using the NRCWE small rotating drum and the INRS Vortex shaker
>
> D4.7: Hydrochemical reactivity, solubility, and biodurability of NANOGENOTOX nanomaterials.

The deliverable 4.7 report presents the results from analysis of the NM hydrochemical reactivity, solubility and inferred biodurability in the NANOGENOTOX 0.5% BSA batch dispersion medium and two synthetic biological media relevant for assessing the NM behavior in the lung-lining fluid (low-Ca Gambles solution) and the intestinal system (Caco 2 cell medium). All three media are relevant for the toxicity testing in the NANOGENOTOX project and the general behavior of MN in biological (test) systems.

Data on the hydrochemical reactivity of MN and their biodurability may be important to better understand the biochemical reactivity of NPs and dissolution in contact with specific biofluids. We may consider a number of reactions taking place when particles come in contact with biofluids. It may cause e.g, changes in pH, adsorption of ions or biomolecules, dissolution, and electron loss or gain, which can result in formation of ROS (reactive oxygen species). ROS are potentially generated during particle-liquid interaction and is often considered as one of the most important parameters of hydrochemical reactivity (e.g., Dick et al., 2003; Xia et al., 2006).

Biodurability is another classical biological test. It was originally established to analyze the degradation (dissolution) rate of asbestos, minerals and man-made fibers in synthetic lung-fluids (e.g., Forster and Tiesler, 1993; Christensen et al., 1994; Sebastian et al., 2002). Lately, the development of biodurability testing has gained new interest with respect to assess the potential residence time of particles in specific compartments of the respiratory, gastro-intestinal or intracellular location as well as mechanistic questions as addressed above (Wiecinski et al., 2009; Xinyuan et al., 2010; Osmond-McCloud et al., 2011; Cho et al., 2011).

The system for determination of biodurability principally consists of a dissolution vessel or membrane chamber, where the analyses may be done in either static or a dynamic liquid flow-through set-up. The temperature, atmosphere conditions in the dissolution vessel are maintained by the use of thermostats (37°C) and continuous air-flow of a specific atmosphere composition (usually 5% CO_2 v/v for lung lining fluids). The biodurability is then quantified by mass-loss determined by collection on filters, usually combined with chemical analysis of the solute.

According to typical standard protocols, the pH is to be maintained by daily manual acid/base adjustments. However, as we show in this work, pH could vary significantly within short time-frames, which can lead to long periods during the test where the pH was far outside the target conditions for e.g., lung lining fluids (pH = 7.4). Maintenance of proper pH conditions or at least its online measurement is important for proper assessment of the biodurability (dissolution/stability) and behaviour of a particulate matter in the specific biological compartments.

Quantification of biodurability is usually done by weighing residual particles on a filter sample and/or measurement of specific constituent elements, which may be online. However, in the analysis of MN biodurability and metal leaching, both particle penetration and loss from test volume by adsorption to membranes might be a risk in case of testing nanoparticles in dynamic flow-through systems. Moreover, representative retrieval of MN from, at least small volume, dispersions, may be associated with some difficulty. Hence, in the interest of improving the test procedures and our understanding of the acute particle-medium (hydrochemical) reactions in air-ways, as well as to ensure that the experimental conditions and test materials are maintained in the test medium, a test-system could include two alternative paths such as:

1) A tier 1, batch dissolution tests of hydrochemical reactivity and solubility under external environmental control mimicking in vitro toxicological test conditions.
2) A tier 2, direct atmosphere-, Temperature- and pH-controlled batch dissolution tests of hydrochemical reactivity and solubility mimicking the conditions in specific biological compartments and the target toxicological test conditions.

Two such systems were also considered for the tests in NANOGENOTOX. First, for tier 2, we attempted using a home build Atmosphere-Temperature-pH-controlled Stirred batch Reactor system (ATempH SBR), previously described in the SOP-report D4.3 (Jensen et al., 2011b). It has reached proof of concept as part of joint support from ENPRA, HINAMOX, NANOGENOTOX and the Danish NANOKEM project, which all had this aim as a minor activity. However, the system had certain time-consuming development needs, including methods optimization for inline Dynamic Light Scattering measurements, high-level pH control, and improved gas flow-control systems, which has yet not been fully resolved for all selected test conditions. A downside compared to the high level of parametric control (atmosphere, temperature, pH) in the ATempH SBR, is that the procedure is relatively slow (at least 24-hour per sample) when only one system is available.

Therefore, we focused on the tier 1 strategy, testing the feasibility of using a commercial 24-well pH and O_2 Sensor Dish Reader (SDR) system, which can be used for testing several samples simultaneously under external environmental control. Pre-tests suggested feasibility with the system and it has now been applied in NANOGENOTOX as well as the EU FP7 projects ENPRA, NANODEVICE and HINAMOX for testing the 24-hour particle pH and O_2 reactivity and solubility under *in vitro* exposure conditions. These results from these tests also suggest proof of concept.

The SDR system enables contemporaneous measurement in 24 wells and therefore greater ability to test several samples per run and to establish a variety of data as function of dose and time. The test

5

conditions using the SDR system are maintained by a cell-incubator and consequently directly corresponds to the conditions of a given *in vitro* exposure event (here 37°C and 5% CO_2 for lung conditions. However, despite the general applicability of the SDR system, the measurable pH-range is only from pH 5 to 9. Therefore, lysosome and gastric systems cannot be studied using this technology. The O_2 concentrations can be measured from 0 to 250% O_2 saturation (0 to 707.6 µmol/l). Due to the principle link between electron activity and oxygen fugacity (e.g., Nordstöm and Munoz, 1994), the variation in O_2 may correspond to values obtained by direct redox potential measurement as used in the ATempH-SBR. However, these potential links must be verified in the future.

As a final output, from the SDR studies, we report the measured amount of soluble MN (concentrations of dissolved elements) after the 24-hour incubation in each of the three incubation media. For this, liquid samples were carefully extracted, filtered and centrifuged to clean out dispersed MN in the liquid sample. Quantification was done as a commercial service without further acid treatment than stabilization. The concentrations of dissolved elements give indication on the durable fraction in the three media. However, in this project, this value can only be indicative as high-precision analysis were not completed on TiO_2 and SAS, and for MWCNT, the associated catalyst particles are probably not good indicators for the durability of the MWCNT.

Appendix A describes the full protocol for running experiments with the SDR system. Off-course the applied SDR procedure is still in the virgin state, but the results have been found promising and the procedure will be put forward for additional protocol development in the EU FP7-project NANoREG.

2 Nanomaterials and information given by suppliers

The tested NANOGENOTOX materials include 6 titania-based (TiO$_2$) products, 5 synthetic amorphous silica (SAS) products and 6 multi-walled carbon nanotubes (MWCNT) (Table 2.1). In NANOGENOTOX, Synthetic Amorphous Silica is described as SAS or SiO$_2$.

Table 2-1 Nanomaterials included in the NANOGENOTOX project and information given by suppliers.

Code	Special notes	Phase	application	Purity wt%	Particle size	BET (m^2/g)	impurity / coating
NM-100	Dry-milled	Anatase	paper loadings, rubber, cosmetics, adhesives, low cost interior paints	98.5	200-220 nm	-	-
NM-101		Anatase	semiconductor catalyst for use in photocatalytic processes	91(99)*	< 10 nm	>250	9%*
NM-102		Anatase	photocatalytic	95	-	90	-
NM-103	hydrophobic	Rutile	cosmetics (sun care, colour), pharma, food	89	20 nm	60	Al2O3 6%, silicone - Dimethicone 2%
NM-104	hydrophilic	Rutile		90	20 nm	60	Al2O3 6% - Dimethicone 2%
NM-105		rutile/anatase	catalysis, heat stabilizer	-	21 nm	50+/-15	-
NM-200	precipitated	PR-A-02	food, processing	-	15 um	220	10 SiO2 1 H2O, 2% soluble salts
NM-201	precipitated	PR-B-01	reinforcement, mechanical and optical properties and process	-	-	160	10 SiO2 1 H2O, 1,5% soluble salts
NM-202	thermal	PY-AB-03	inks, adhesives, cosmetics, reinforcement, powder process, food, pharmaceuticals	>99,8	-	170-230	-
NM-203	thermal	PY-A-04	food, cosmetics pharma, reinforcement	-	12 nm	200+/-25	hydrates?
NM-204	Precipitated		food	-	-	140	-

* calcination causes loss of 9 wt% and the residual is 99% pure

7

www.nanogenotox.eu

Co-funded by
the Health Programme
of the European Union

Code	Special notes	Phase	application	Purity wt%	CNT tube length	BET (m^2/g)	impurity / coating
NM-400	CCVD	MWCNT	structural composite and energy applications	-	~1.5 um long	250-300	10 wt% oxides/coated with pyrogenic carbon
NM-401	CCVD	MWCNT	structural composite and energy applications	-	5-15 um long	40-300	~2% amorph. carbon
NM-402	CCVD	MWCNT	structural composite and energy applications	-	0.1-10 um long	-	<10 wt%
NM-403	CCVD	MWCNT	structural composite and energy applications	-	1->10 µm long	-	-
NRCWE-006	CVD	MWCNT	energy / Li-ion battery	>99.5	segments; 3-5 um long	24-28	
NRCWE-007	CCVD	MWCNT	structural composites etc.	-	8-15 nm OD; 10-50 um long	233	ca. 3.2 wt% C impurties/ < 1.5wt% ash (Al, Cl, S)

Co-funded by
the Health Programme
of the European Union

3 Experimental procedures

3.1 Hydrochemical reactivity, solubility, and biodurability

The acute hydrochemical MN reactivity, solubility and biodurability was assessed in the 0.05% BSA batch dispersion medium, low-Ca Gamble's solution, and in Caco 2 cell medium by 24-hour incubation at $37^{\circ}C$ and $5\%CO_2$ air at 95% RH in a cell incubator. Dispersions were prepared as described in the generic NANOGENOTOX dispersion protocol to mimic the treatment used for toxicological studies (Jensen et al., 2011a).

3.1.1 The Sensor Dish Reader (SDR) system

The hydrochemical reactivity was assessed regarding acid-base reactivity and influence on the oxygen balance using a recently developed 24-well SDR (Sensor Disc Reader) system (PreSens Precision Sensing GmbH, Germany) intended for use for in vitro assays (Figure 3.1). Determination of the acid-base reactivity is particularly important in cell media, where a buffer usually is applied to ensure pH stability in the bioassay. However, if a NM is particular reactive, this pH buffer may be insufficient at sufficiently high NM doses. The O_2 reactivity may another important parameter and relates to hydrochemical reactions that consume or liberate oxygen. Deviations in the O_2-balance can be caused by different reactions including redox-reactions, protonation and deprotonation in the dispersion. These phenomena may be caused by catalytic reactions, but also dissolution, transformation of molecular speciation and precipitation in the medium under investigation.

Figure 3.1. SDR Sensor Dish Reader, examples of sensor products and illustration of the SDR measurement principle. In this study we used the 24-well Oxy- and HydroDish for O_2 and pH monitoring, respectively. Source: PreSens Precision Sensing GmbH, Germany.

The pH variation was measured using the HydroDish® fluorescent sensor plate for pH detection with up to ± 0.05 pH resolution for pH 5 to 9. Measurement is not possible outside of these ranges.
The O_2 variation was measured using the OxoDish® fluorescent sensor plate for O_2 detection with ± 2 % air saturation resolution. The OxoDish® sensor can measure O2 concentrations between 0 and 250% saturation, corresponding to 0 to 707.6 µmol/l.

In brief the fluorescent sensors spots are placed at the bottom of each of the wells in the dishes. For our study, we used 24 well plates. The sensor spot contains a luminescent dye. It is excited by the SensorDish® Reader using a laser diode, placed below the multidish. The diode is only active when analyses are done, and the sensor luminescence lifetime is detected through the transparent bottom. The luminescence lifetime of the dye varies with the oxygen partial pressure (OxoDish®) and the pH of the sample (HydroDish®), respectively. This signal is converted to oxygen and pH values by the instrument software. The sensor plates are pre-calibrated and these calibration data are uploaded and used for the specific plates used.

3.1.2 Experimental procedure

Samples were prepared by prewetting all MN with 0.5% v/v ethanol and dispersion in 0.05% w/v BSA water by probe-sonication following the generic NANOGENOTOX dispersion protocol (Jensen et al., 2011a). Chemically pre-analyzed and approved Nanopure filtered water was used for the batch dispersion to ensure minimum background contamination in the test.

The incubation media included 0.5% BSA-water, low-Ca Gambles solution and Caco 2 medium. The BSA water was included in the study to assess the behavior of the MN in the batch dispersion medium, which is the first stage in all the biological tests in NANOGENOTOX. The reactivity was tested at doses 0.32, 0.16, 0.08 and 0 mg/ml and a total volume of 2 ml was entered into each well of the SDR plates. Figure 3.2 illustrates the general procedure.
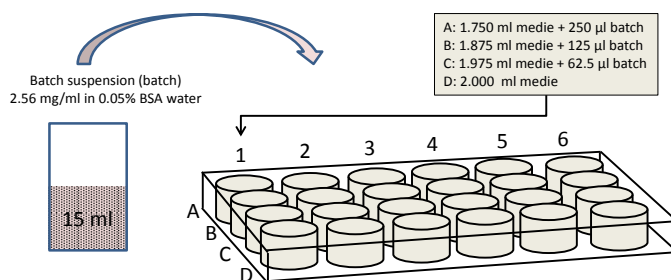

Figure 3.2: Principal sketch of the dosing into the SDR plates resulting in 2 ml test medium in each well. In this way six dose-response measurements can be made in one test round.

After 24-hours incubation, the maximum dose and control media from the pH and O_2 wells were retrieved by pipette, filtered through a 0.2 µm CAMECA syringe filter and centrifuged in Eppendorf tubes for 60 minutes at 20,000xG RCF using a Ole Dich table top centrifuge. MN samples were placed in the outer ring and pure reference media in the inner ring. Hereafter, the upper 1.25 ml of each filtrates from the pH and O_2 wells were sampled, pooled (2.5 ml) in Eppendorf tubes and stabilized with 1 ml 2% HNO_3 water (sample diluted 5/7). The liquids were then stored in darkness until send for analyses. All vials were washed and rinsed in acid before use.

A detailed protocol is given in Appendix A.

3.1.3 Data treatment and evaluation

The reactivity of the individual MN was evaluated qualitatively from the evolution of the pH and O_2 over time for each of the MN in each of the four dose levels, including the blank control. The SDR pH-values were plotted directly as function of time. The data were then evaluated visually comparing the SDR values of exposed wells with that of the un-exposed control media as well the readings from the initial medium readings in each of the wells to assess if there would be any systematic off-set in some of the sensors. This sensor-evaluation was always done using the blank control as the assumed correct internal reference value.

For the O_2 analyses, the difference between the time-resolved readings from the "exposure doses" and the medium control ($dO_2 = (O_{2,dose} - O_{2,medium\ contol})$) was plotted as function of time.

For both pH and O_2, if the SDR readings from the dosed media showed no difference or followed the same trend as the reference media, the NM was assumed to have neglible pH reactivity or influence on the oxygen balance through redox reactivity or dissolution.

3.1.4 Nanomaterial dissolution and biodurability

The MN dissolution and biodurability was assessed from elemental analyses of the solute adjusted for background concentrations in the three test media. It was assumed that that maximum dissolution would be observed at the 0.32 mg/ml dose and that equilibrium was reached in 24 hours. Consequently, if the elemental composition of the test materials is given, the results enable calculation of the solubility limit as well as the durability (the un-dissolved residual) of the specific MN in the batch dispersion, the lung lining fluid and the Caco2 media. However, in this study, we have only semiquantitative elemental composition data on the TiO2 and SAS. For MWCNT, the results may be difficult to interpret due to the quantification is made on the associated catalyst tracers, which may very likely behave differently than the MWCNT.

3.1.5 Elemental analysis

The concentrations of dissolved Si elements in the media were analyzed using Inductively Coupled Plasma-Optical Emission Spectroscopy (ICP-OES). Ti, Al, Fe, Co, and Ni were determined by ICP Mass-spectrometry (ICP-MS). Both element series were analysed as a commercial service by Eurofins, DK-6600 Vejen, Denmark. The elemental background concentrations in the three test media was determined on three doublet samples for each media and the elemental concentrations after dissolution were determined in two sub-samples for each MN.

4 Results

4.1 Hydrochemical pH reactivity

Figures 4.1 to 4.16 show the temporal pH evolution in each of the tested MN incubations considering the highest dose experiments compared to the reference (zero-dose). No online data is available on NM-403, where the SDR plates by mistake were placed wrongly on the reader. The results show that most of the MN has negligible to moderate influence on the pH-evolution in the three test media. If there is a significant pH reaction, this normally occurs within the first few hours. However, it is particularly noteworthy, that the temporal evolution follow overall general trends depending on the test medium.

The pH in the 0.05% BSA water batch dispersion medium typically increases from near or below the pH 5 lower detection limit to between pH 5 and 6 within the first hour. Addition of MN to the BSA water appears generally to cause a small elevation in the pH as compared to the reference medium.

The Gambles solution medium has slightly basic pH values, typically starting between pH 8 and 9. In a few cases, the pH even exceeds the pH 9 upper detection limit of the SDR even from the beginning or during the experiment (e.g., Figure 4.5b and 4.7b). This clearly demonstrates there may be a need to perform accurate online pH control to avoid episodes with unrealistic biological simulation or test conditions. Moreover, the protocol should ensure that pH adjustment in this type of static experiment without online pH control at least make proper pH adjustment in the initial step of the test. This is clearly specified in the protocol in Appendix A.

The Caco 2 cell medium normally has an initial pH around 7.5 to 8 and the pH, except for a few cases, normally drops slightly during the 24-hour experiment. In the test with NM-200 (Figure 4.7c), the pH increases dramatically in all wells from ca. half an hour to almost 2 hours. This was also seen for BSA water and Gamble solution and suggests that a stop or lowering of the CO_2 control may have occurred. The notable increase at the last few hours of testing NM-202 (Figure 4.9) may be due to similar events.

The known presence of organic coatings in NM-103 and NM-104 did not appear to affect the temporal pH evolution notably. Due to the occasional presence of Na_2SO_4 in the SAS samples, some lowering of the pH could be expected for NM-200, NM-201, and NM-202. However, this was not observed. For the MWCNT, the CNT should be in-active towards pH as such, but presence of several catalyst and processing impurities such as chlorides and sulfates, reported for NRCWE-007 could affect pH as well as reaction with catalyst particles. However, only unsystematic potential affects were observed as pH increases over a certain time-interval in e.g., NM-400, NM-401 in BSA water and Caco 2 media, NM-402 in BSA-water and Gambles solution, and NRCWE-007 in Caco2 medium.

As a general conclusion, it is found that the selected incubation media and the incubator atmosphere are the primary controllers of the temporal pH evolution for these MN.
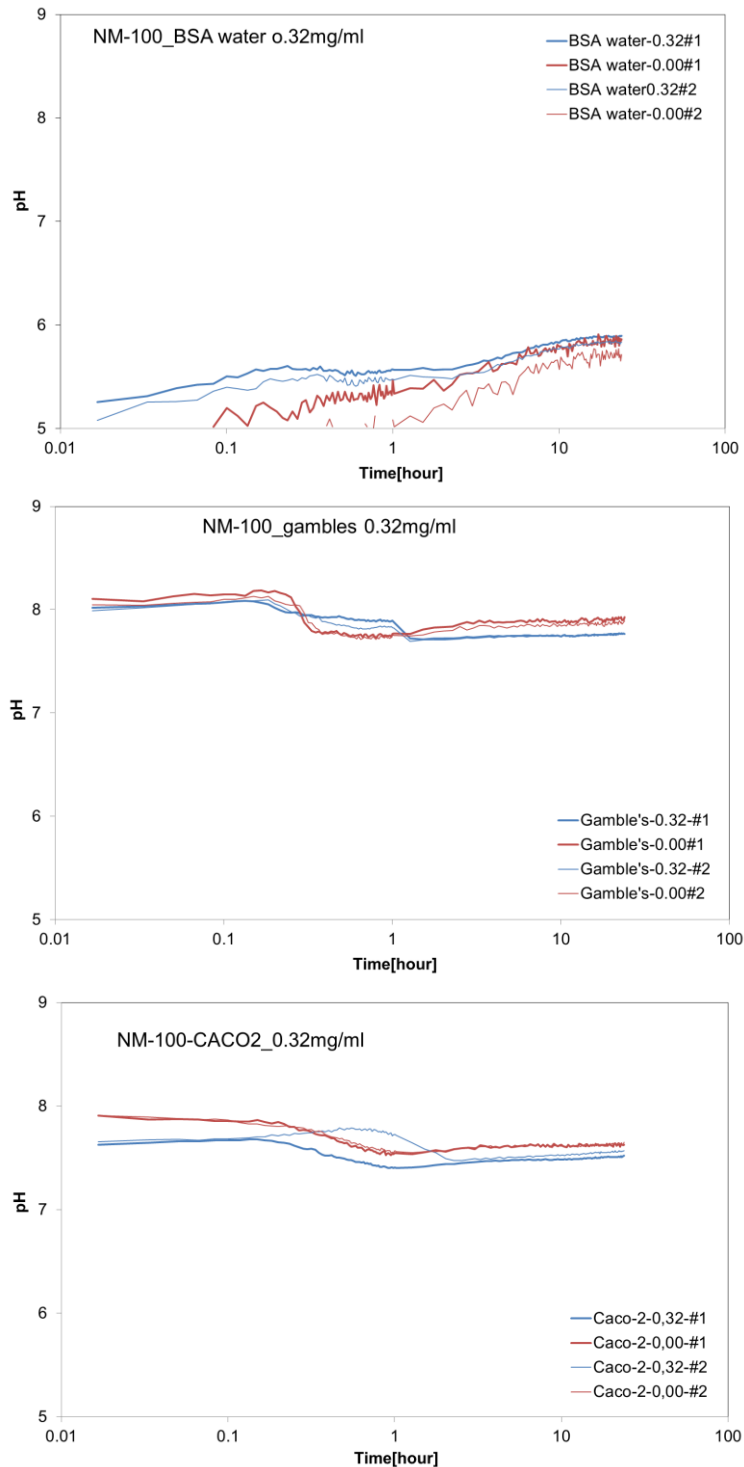
*Figure 4.1. pH-evolution during 24-hour incubation of NM-100 in **a)** 0.05% BSA water NANOGENOTOX batch dispersion; **b)** Gambles solution; and **c)** Caco2 cell medium. The particle concentrations in the Gambles solution and Caco2 cell medium were dosed from the batch dispersion tested in a).*
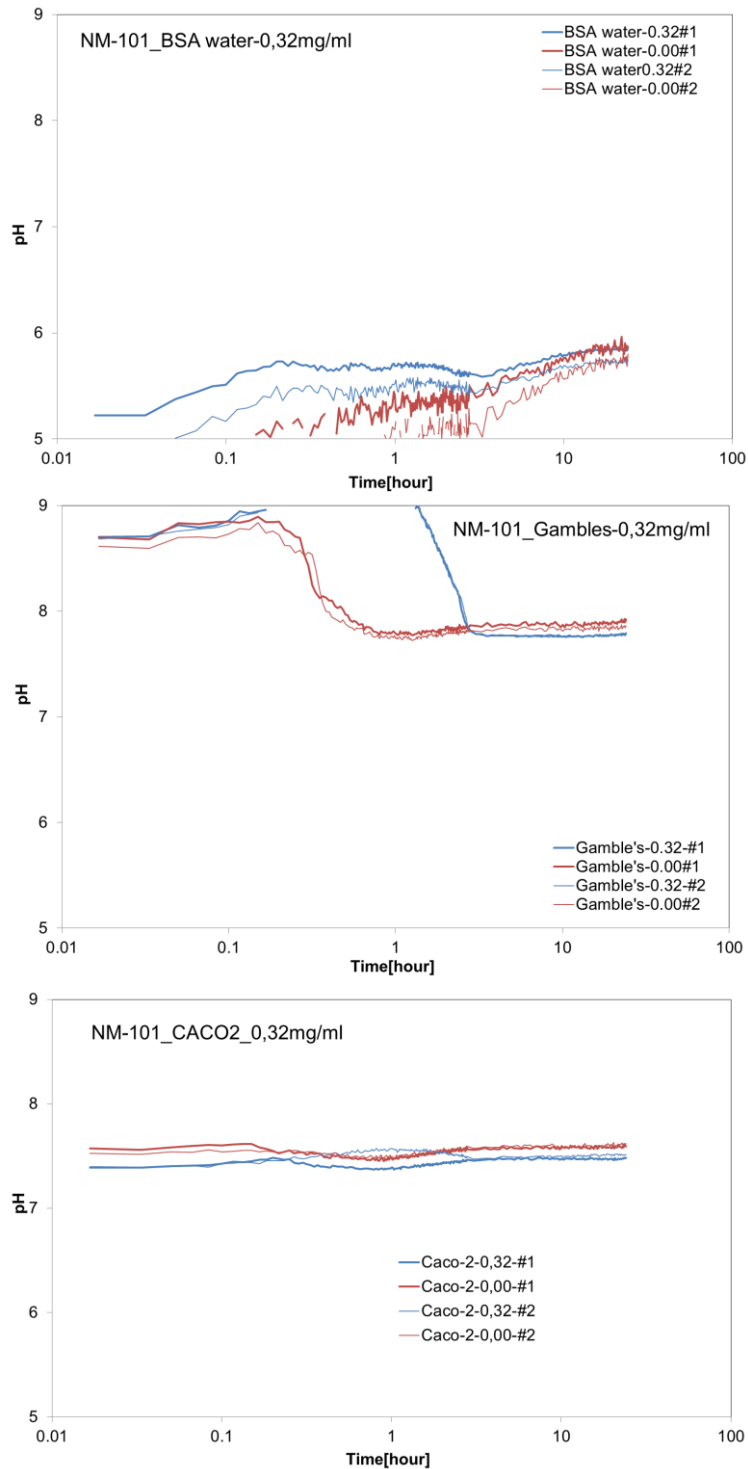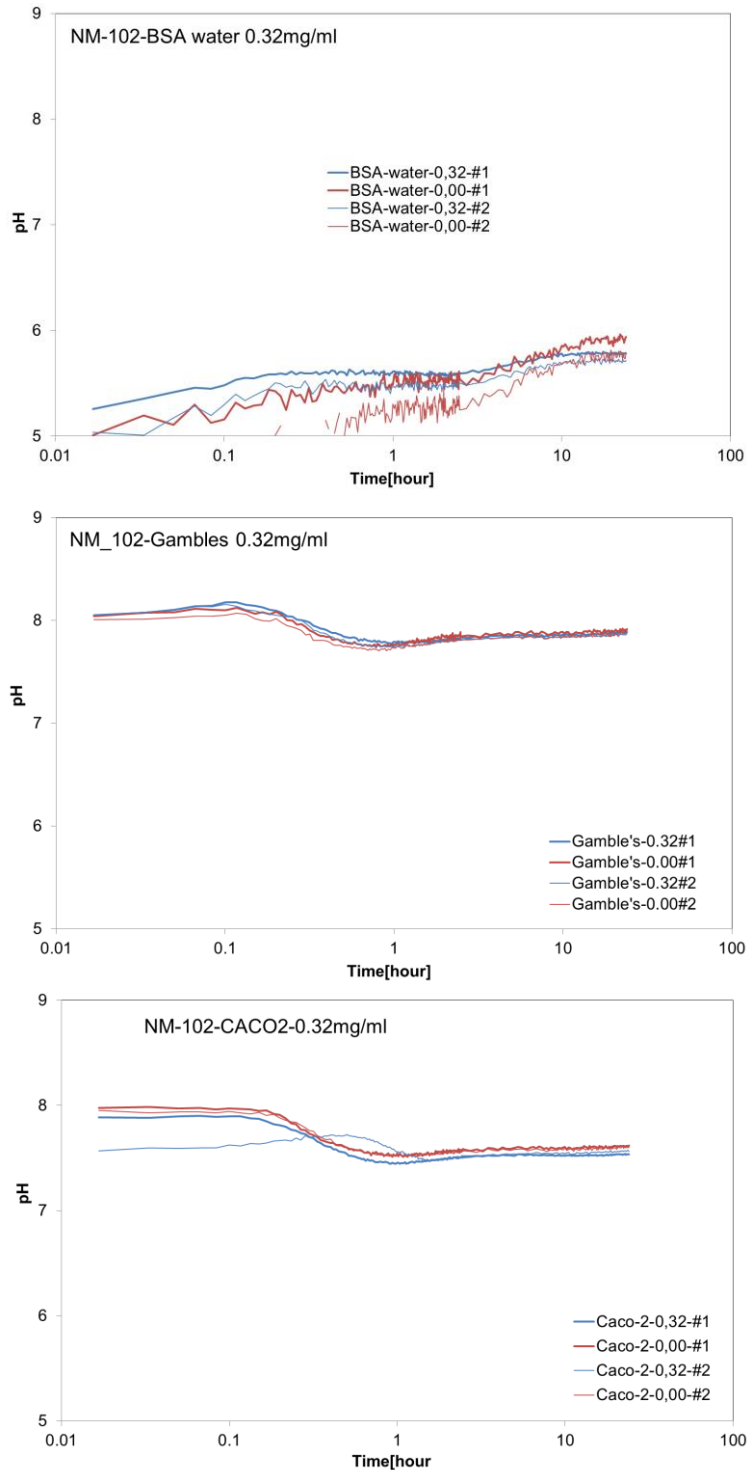
*Figure 4.2. pH-evolution during 24-hour incubation of NM-101 in **a)** 0.05% BSA water NANOGENOTOX batch dispersion; **b)** Gambles solution; and **c)** Caco2 cell medium. The particle concentrations in the Gambles solution and Caco2 cell medium were dosed from the batch dispersion tested in a).*
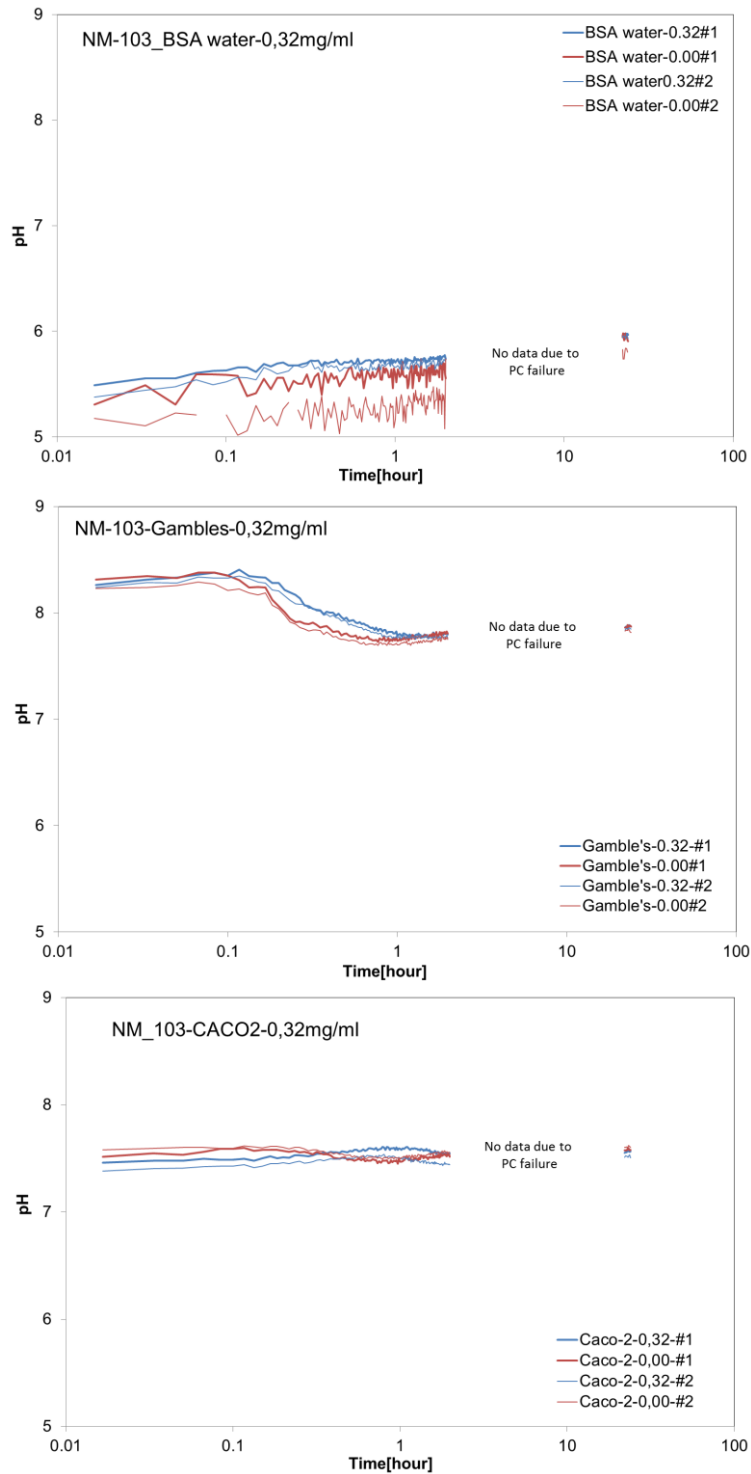
*Figure 4.3. pH-evolution during 24-hour incubation of NM-102 in **a)** 0.05% BSA water NANOGENOTOX batch dispersion; **b)** Gambles solution; and **c)** Caco2 cell medium. The particle concentrations in the Gambles solution and Caco2 cell medium were dosed from the batch dispersion tested in a).*
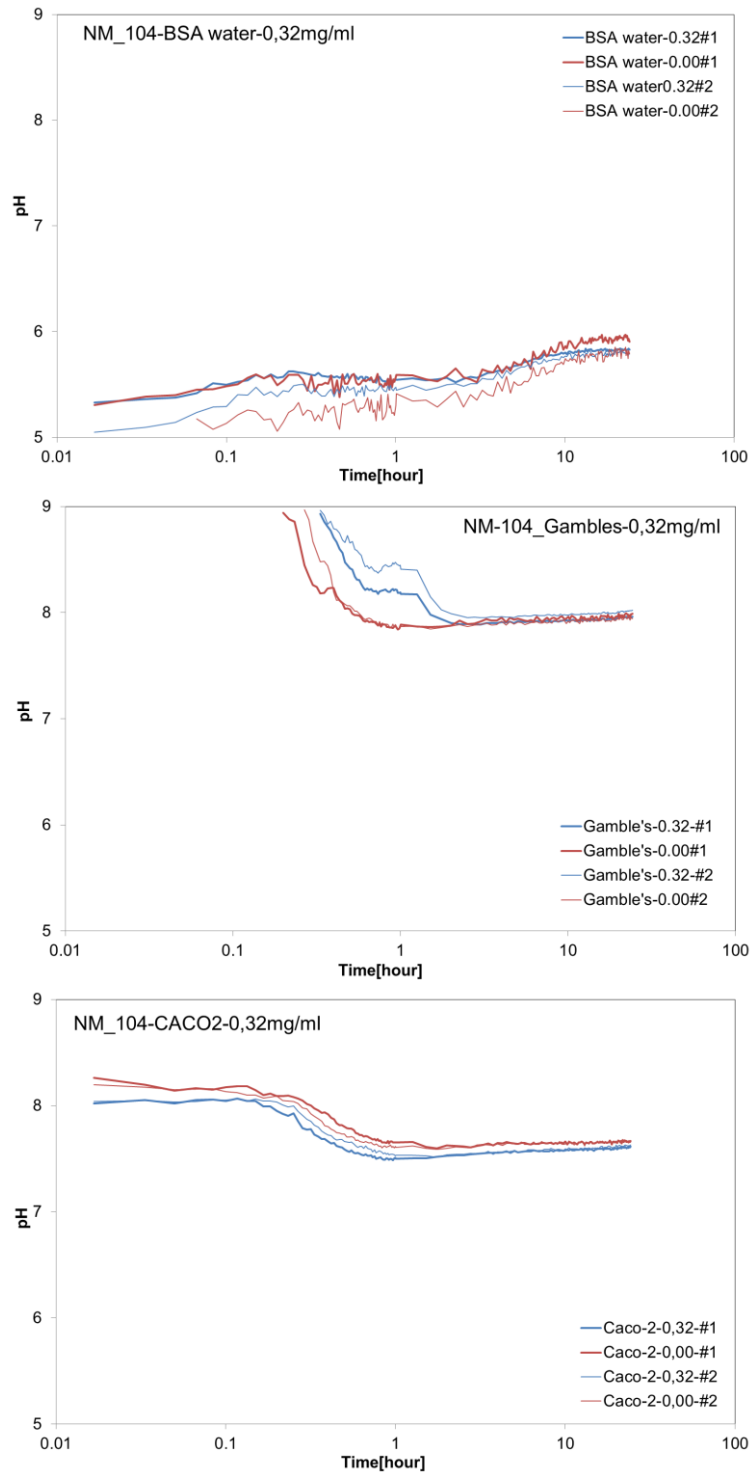
*Figure 4.4. pH-evolution during 24-hour incubation of NM-103 in **a)** 0.05% BSA water NANOGENOTOX batch dispersion; **b)** Gambles solution; and **c)** Caco2 cell medium. The particle concentrations in the Gambles solution and Caco2 cell medium were dosed from the batch dispersion tested in a).*

Figure 4.5. pH-evolution during 24-hour incubation of NM-104 in a) 0.05% BSA water NANOGENOTOX batch dispersion; b) Gambles solution; and c) Caco2 cell medium. The particle concentrations in the Gambles solution and Caco2 cell medium were dosed from the batch dispersion tested in a).

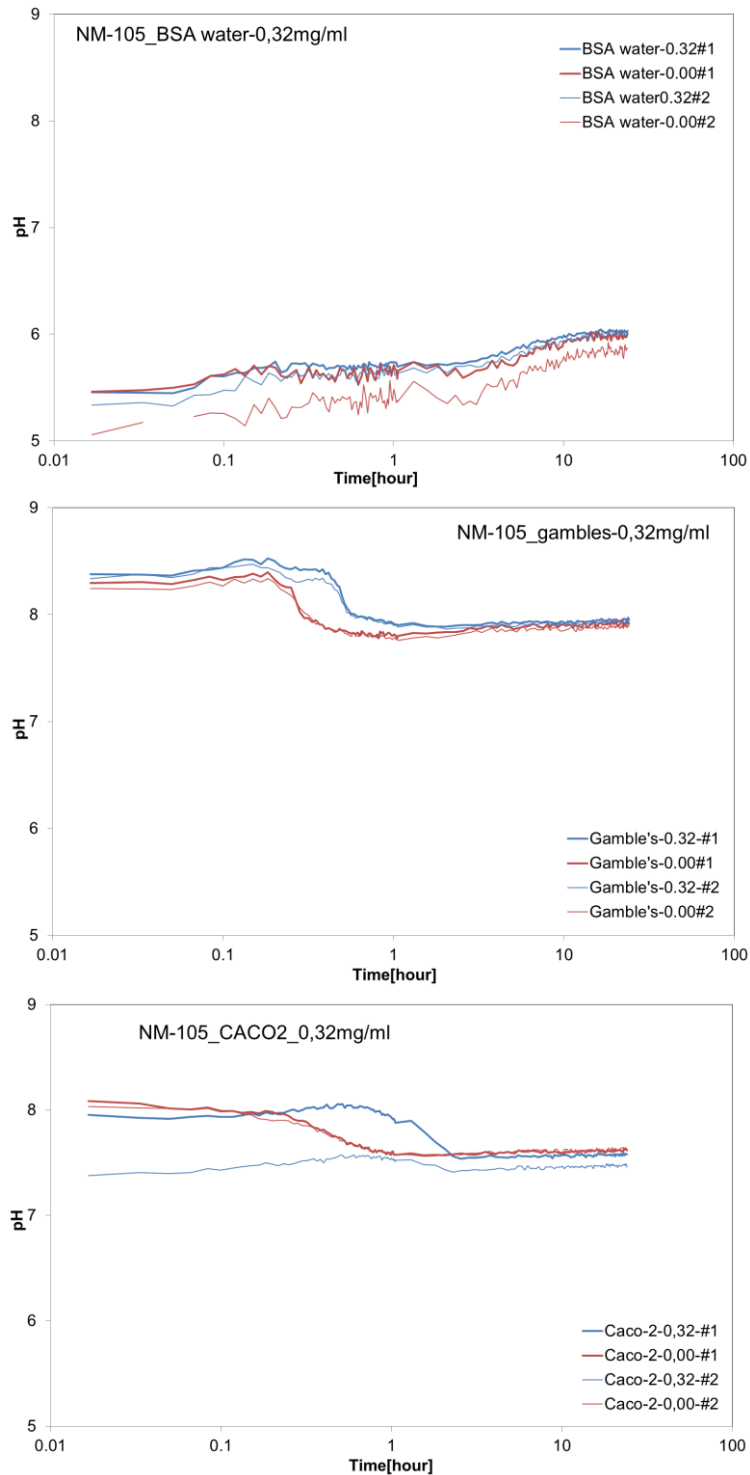*Figure 4.6. pH-evolution during 24-hour incubation of NM-105 in a) 0.05% BSA water NANOGENOTOX batch dispersion; b) Gambles solution; and c) Caco2 cell medium. The particle concentrations in the Gambles solution and Caco2 cell medium were dosed from the batch dispersion tested in a).*

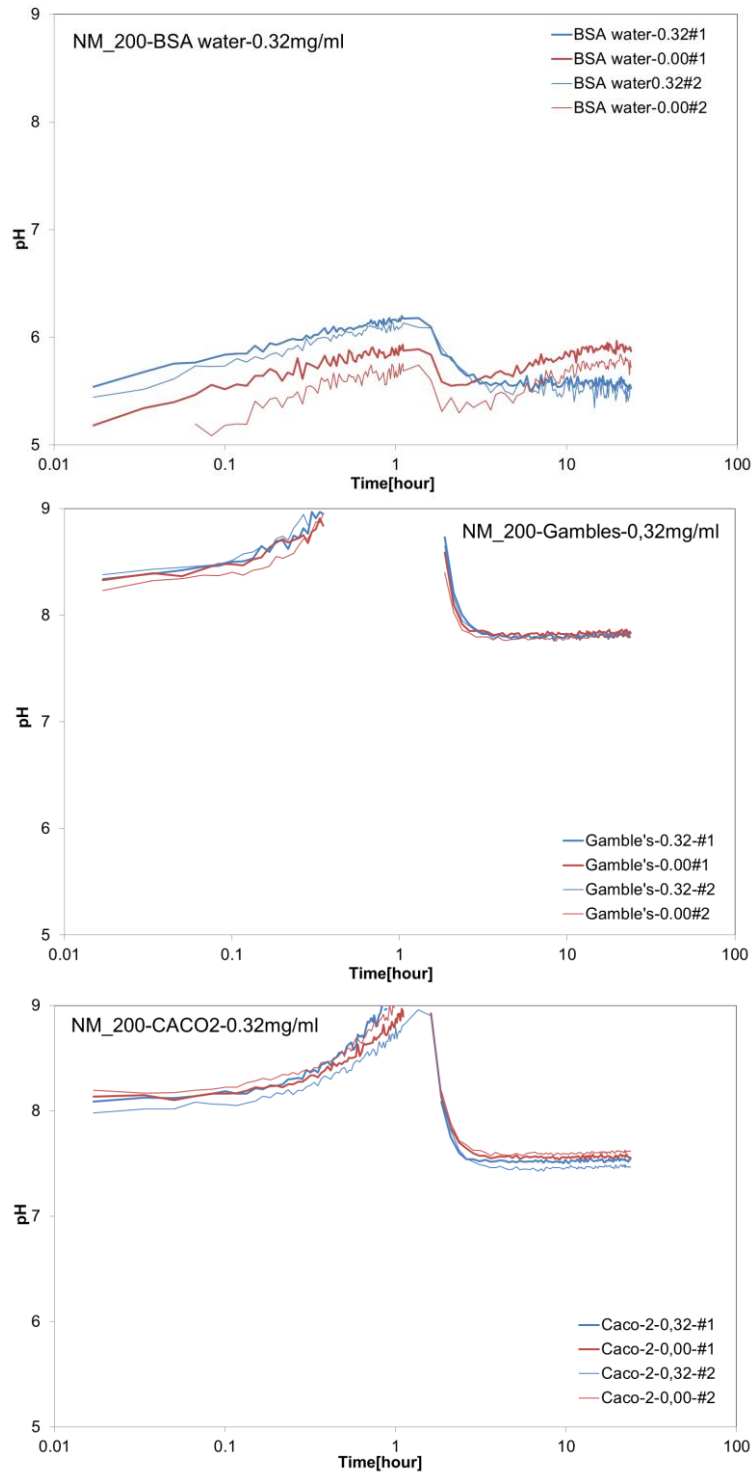*Figure 4.7. pH-evolution during 24-hour incubation of NM-200 in* **a)** *0.05% BSA water NANOGENOTOX batch dispersion;* **b)** *Gambles solution; and* **c)** *Caco2 cell medium. The particle concentrations in the Gambles solution and Caco2 cell medium were dosed from the batch dispersion tested in a).*
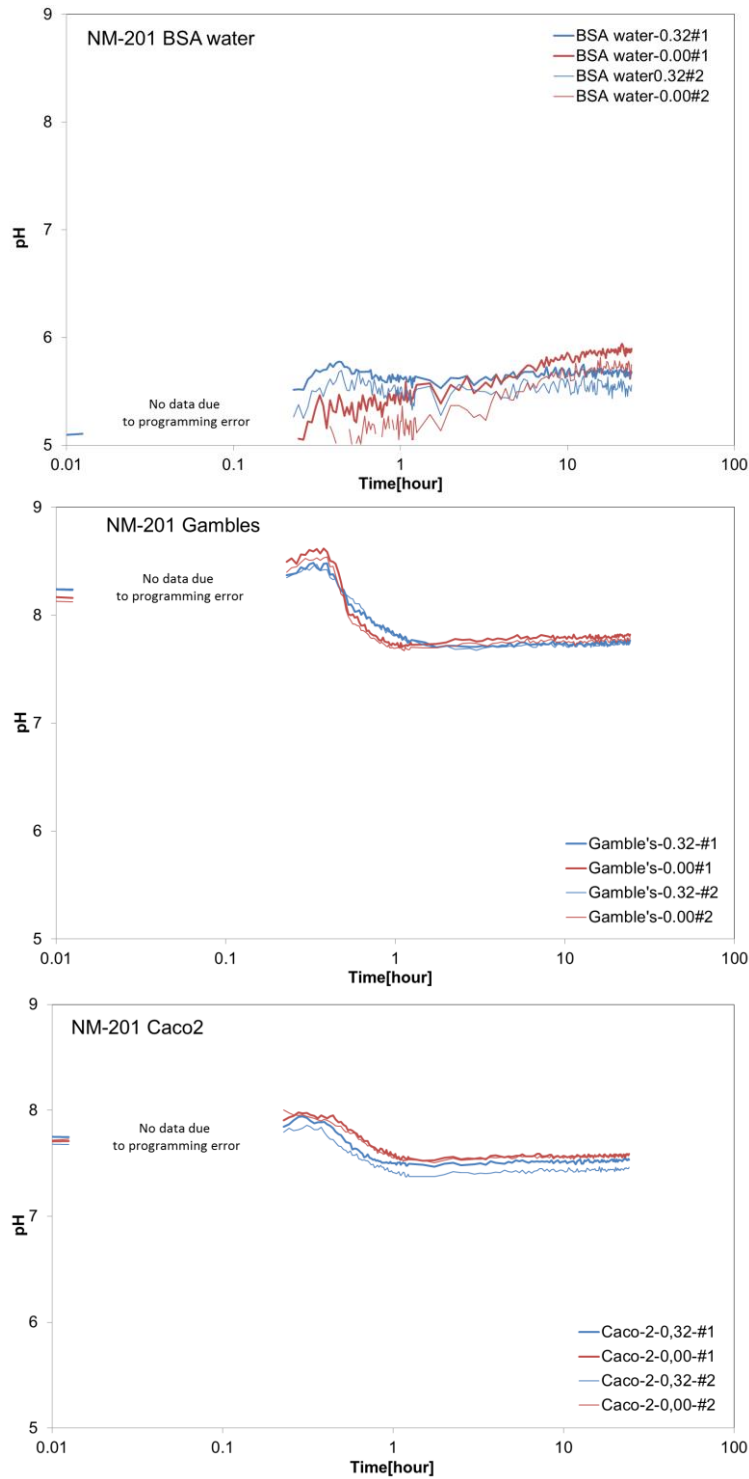
*Figure 4.8. pH-evolution during 24-hour incubation of NM-201 in **a)** 0.05% BSA water NANOGENOTOX batch dispersion; **b)** Gambles solution; and **c)** Caco2 cell medium. The particle concentrations in the Gambles solution and Caco2 cell medium were dosed from the batch dispersion tested in a).*

*Figure 4.9. pH-evolution during 24-hour incubation of NM-202 in **a)** 0.05% BSA water NANOGENOTOX batch dispersion; **b)** Gambles solution; and **c)** Caco2 cell medium. The particle concentrations in the Gambles solution and Caco2 cell medium were dosed from the batch dispersion tested in a).*
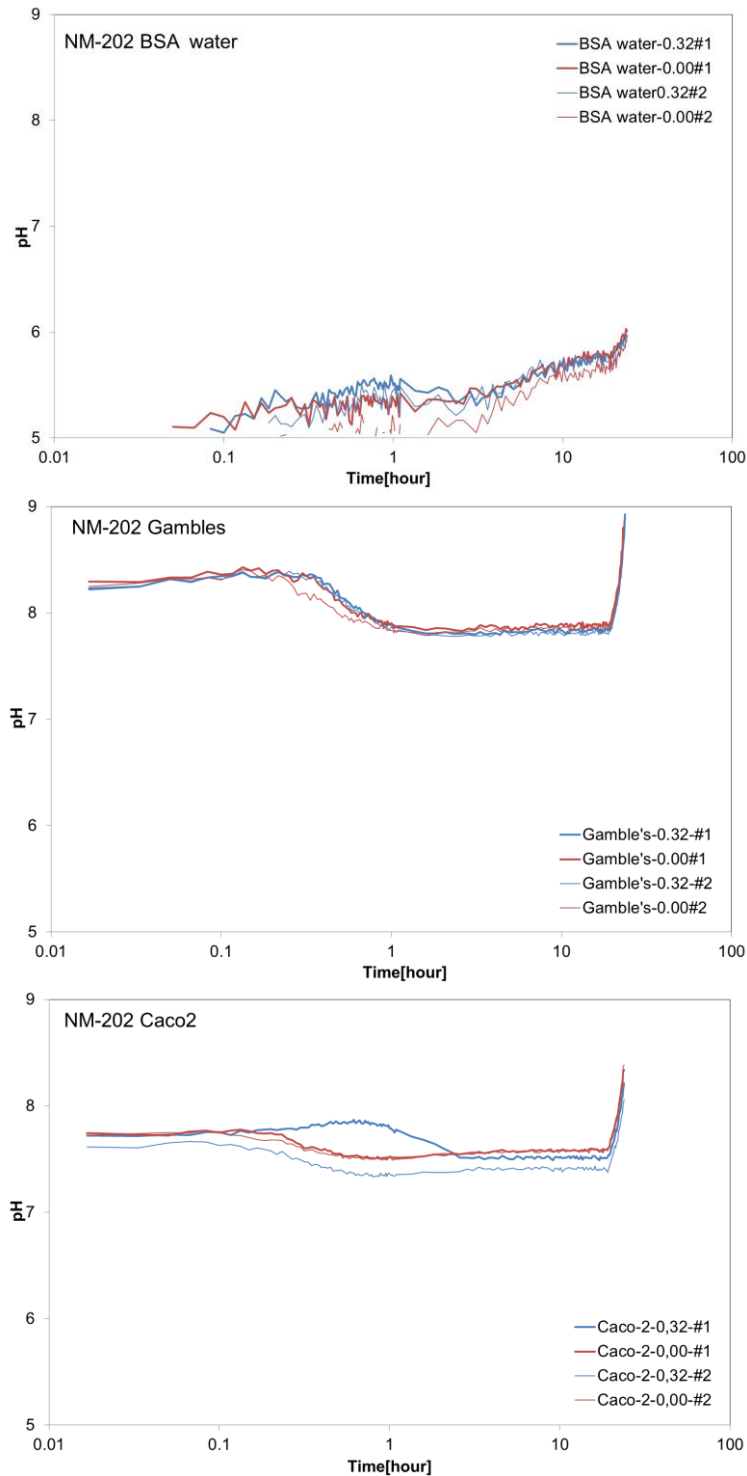
Co-funded by
the Health Programme
of the European Union

*Figure 4.10. pH-evolution during 24-hour incubation of NM-203 in **a)** 0.05% BSA water NANOGENOTOX batch dispersion; **b)** Gambles solution; and **c)** Caco2 cell medium. The particle concentrations in the Gambles solution and Caco2 cell medium were dosed from the batch dispersion tested in a).*

*Figure 4.11. pH-evolution during 24-hour incubation of NM-204 in **a)** 0.05% BSA water NANOGENOTOX batch dispersion; **b)** Gambles solution; and **c)** Caco2 cell medium. The particle concentrations in the Gambles solution and Caco2 cell medium were dosed from the batch dispersion tested in a).*
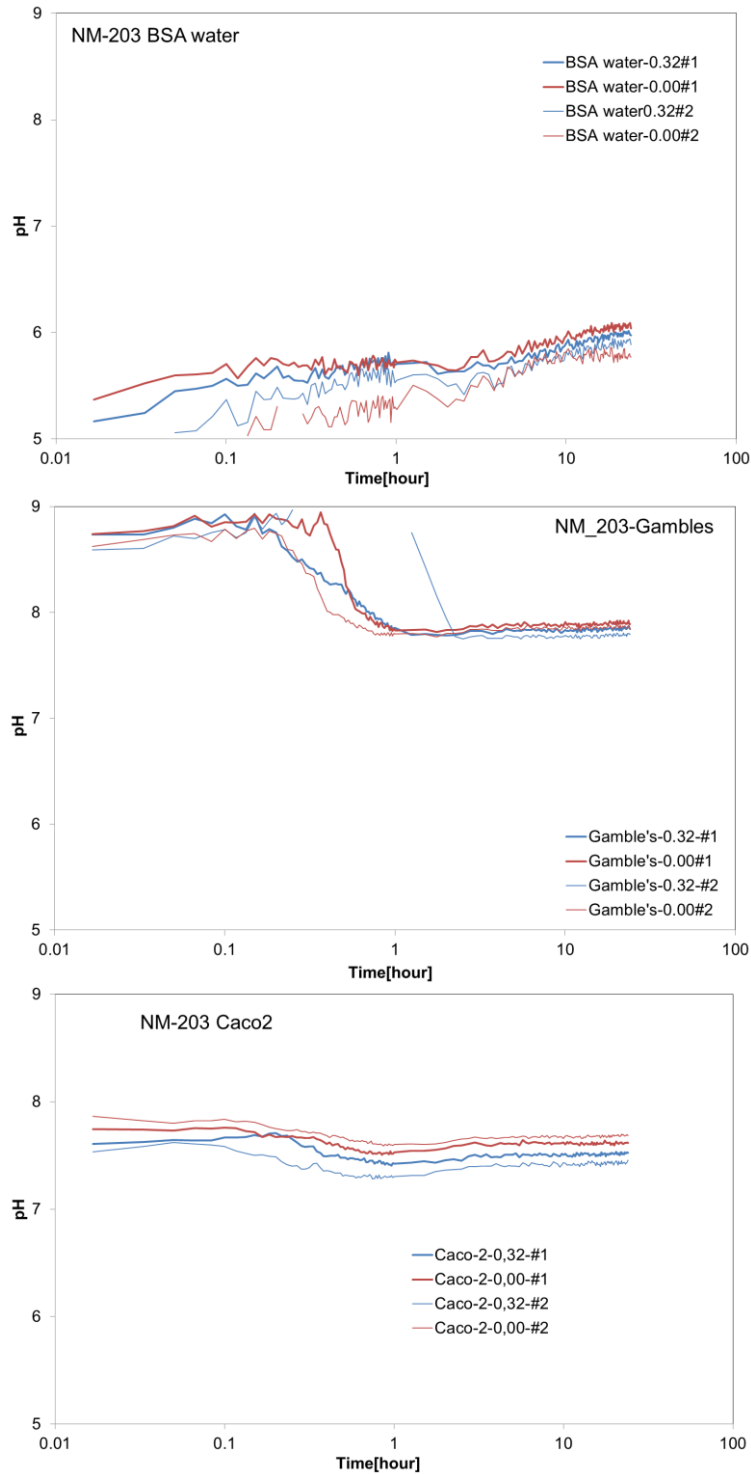
Figure 4.12. pH-evolution during 24-hour incubation of NM-400 in a) 0.05% BSA water NANOGENOTOX batch dispersion; b) Gambles solution; and c) Caco2 cell medium. The particle concentrations in the Gambles solution and Caco2 cell medium were dosed from the batch dispersion tested in a).

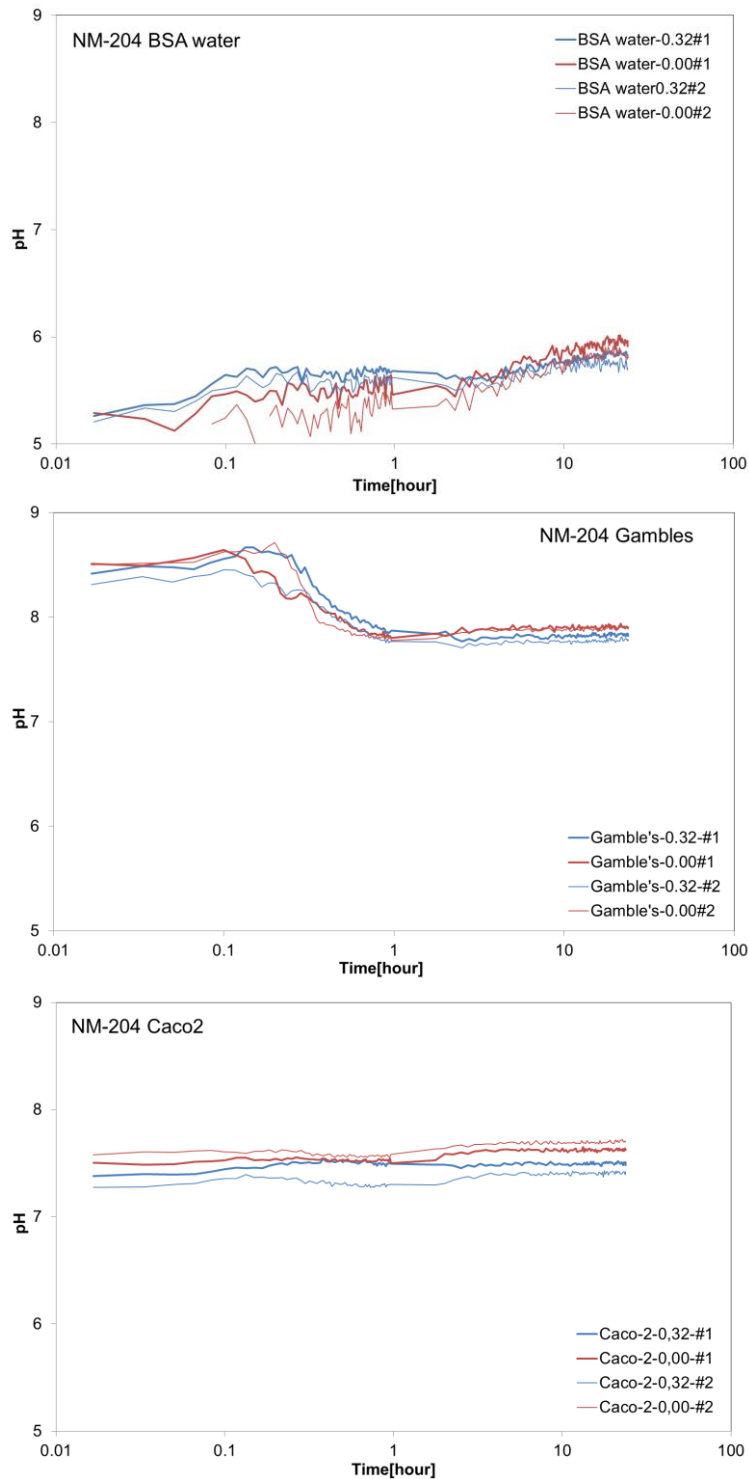*Figure 4.13. pH-evolution during 24-hour incubation of NM-401 in a) 0.05% BSA water NANOGENOTOX batch dispersion; b) Gambles solution; and c) Caco2 cell medium. The particle concentrations in the Gambles solution and Caco2 cell medium were dosed from the batch dispersion tested in a).*

*Figure 4.14. pH-evolution during 24-hour incubation of NM-400 in **a)** 0.05% BSA water NANOGENOTOX batch dispersion; **b)** Gambles solution; and **c)** Caco2 cell medium. The particle concentrations in the Gambles solution and Caco2 cell medium were dosed from the batch dispersion tested in a).*
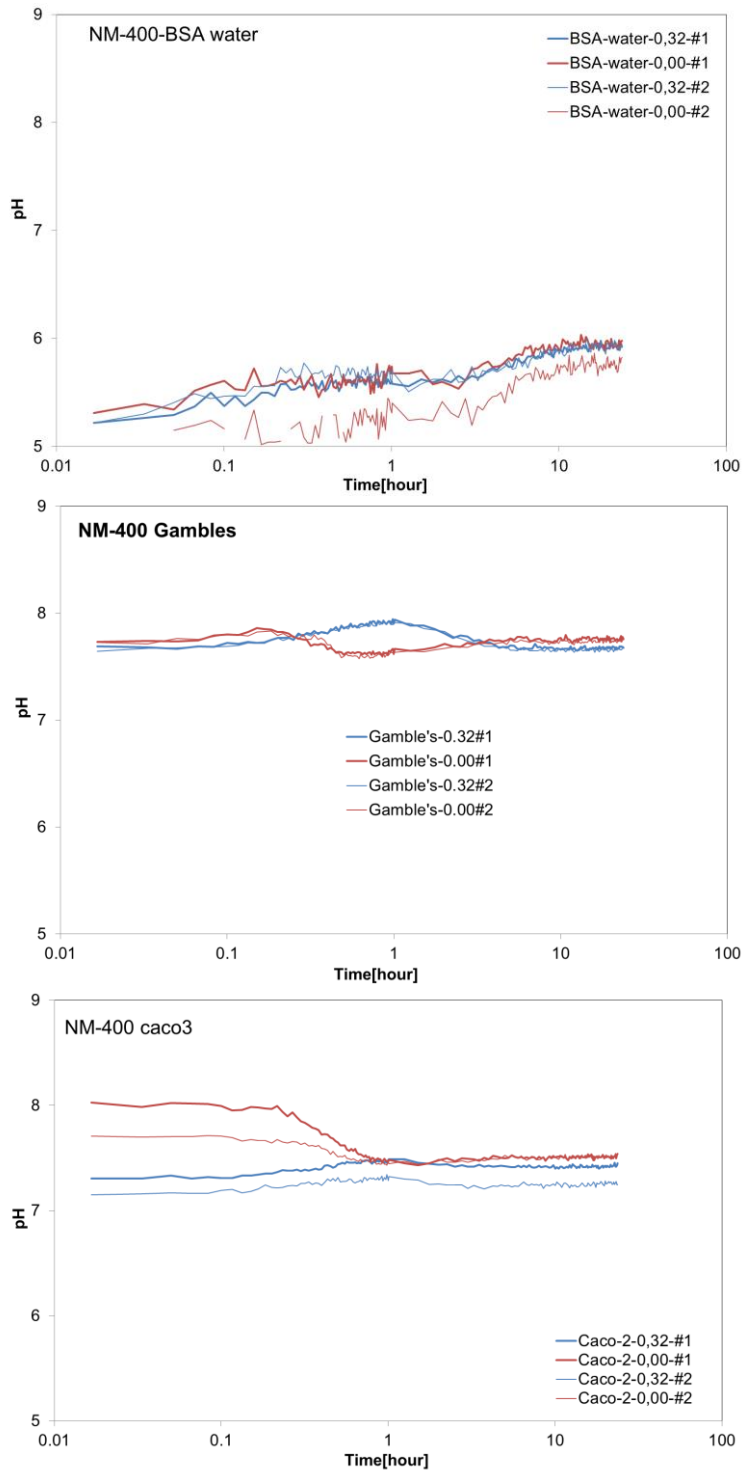
Figure 4.13. pH-evolution during 24-hour incubation of NRCWE-006 in a) 0.05% BSA water NANOGENOTOX batch dispersion; b) Gambles solution; and c) Caco2 cell medium. The particle concentrations in the Gambles solution and Caco2 cell medium were dosed from the batch dispersion tested in a).
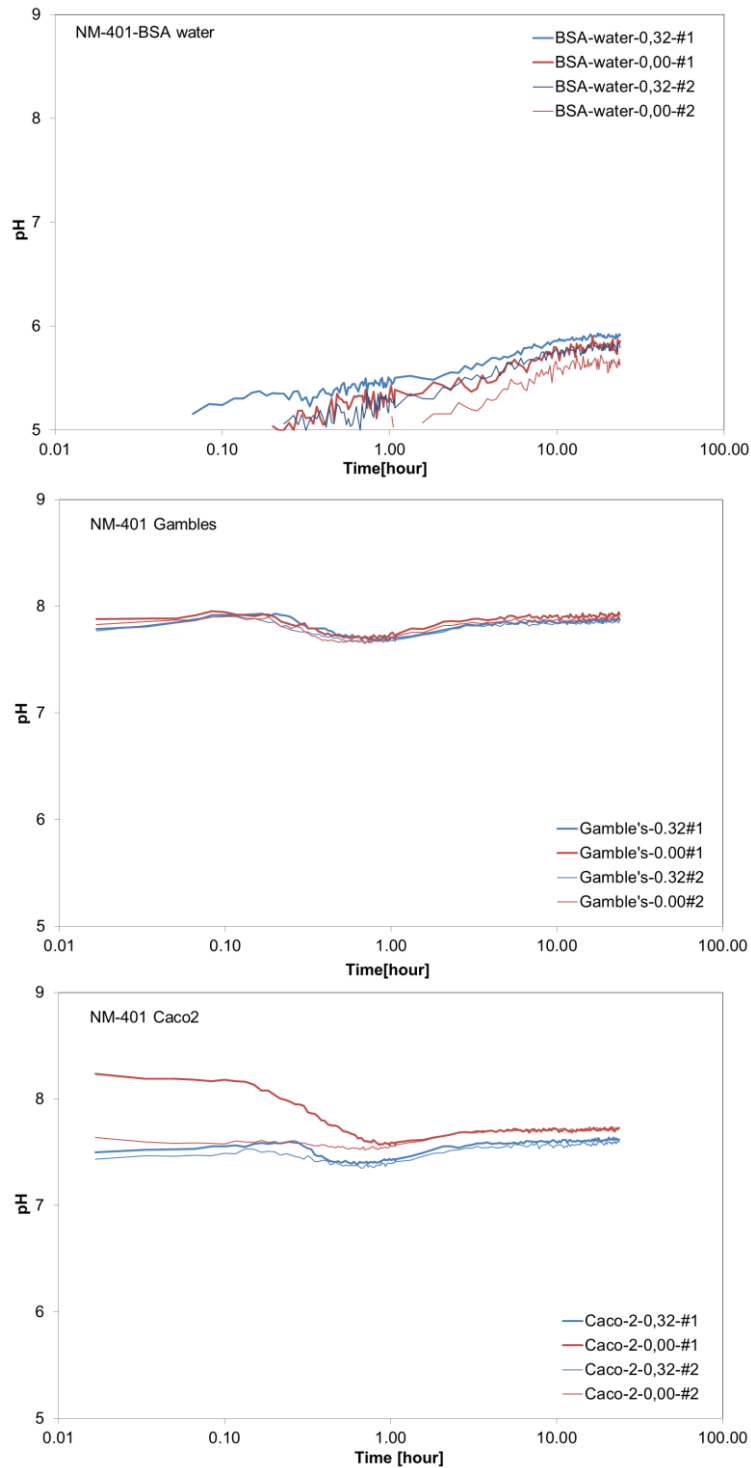
*Figure 4.14. pH-evolution during 24-hour incubation of NRCWE-007 in **a)** 0.05% BSA water NANOGENOTOX batch dispersion; **b)** Gambles solution; and **c)** Caco2 cell medium. The particle concentrations in the Gambles solution and Caco2 cell medium were dosed from the batch dispersion tested in a).*
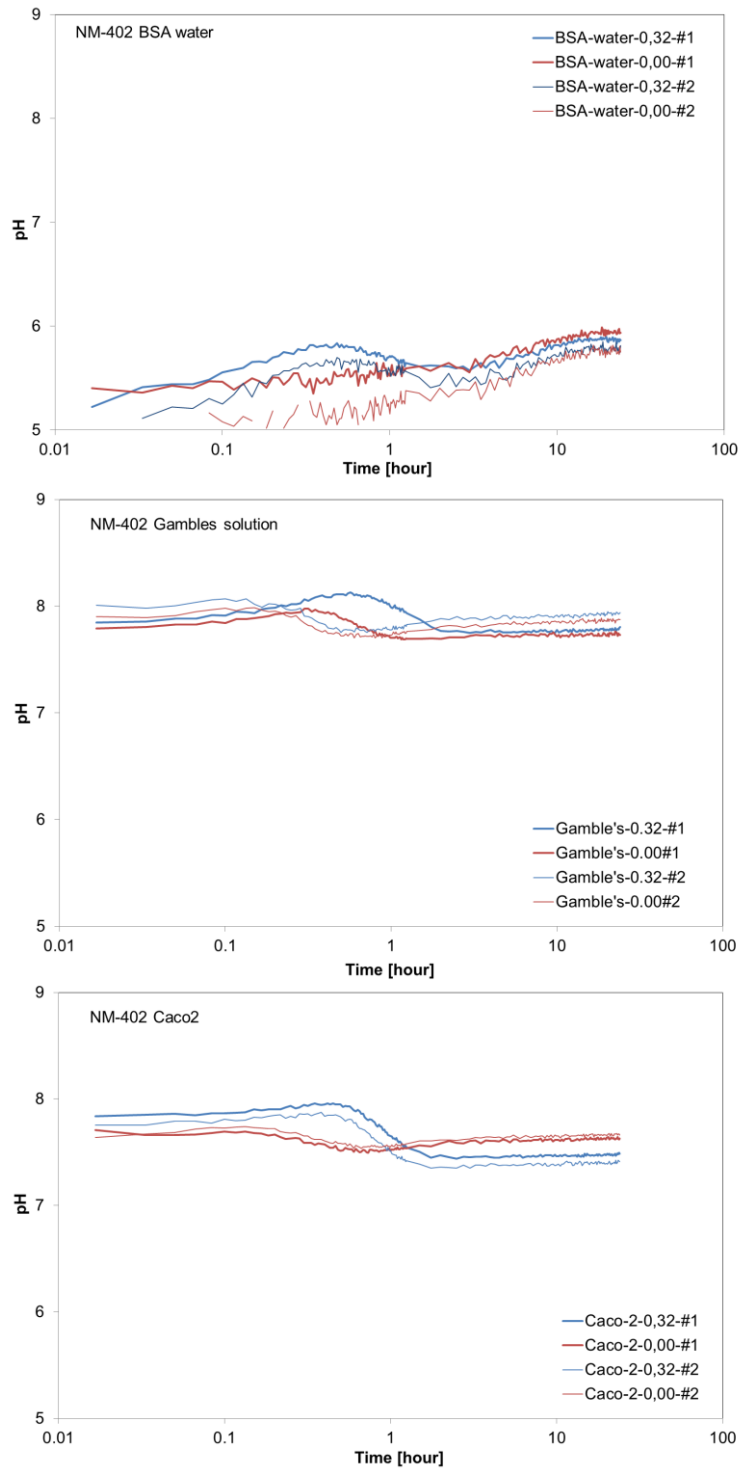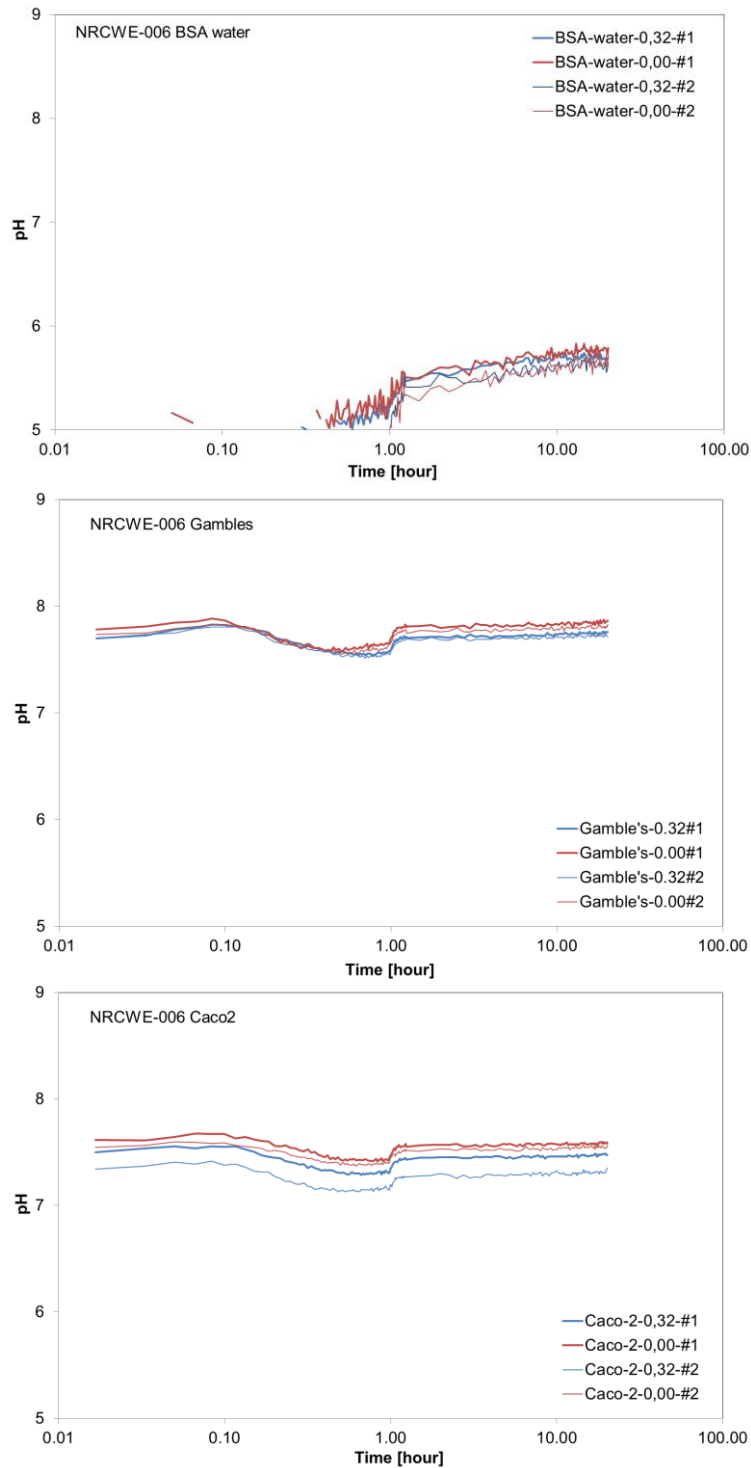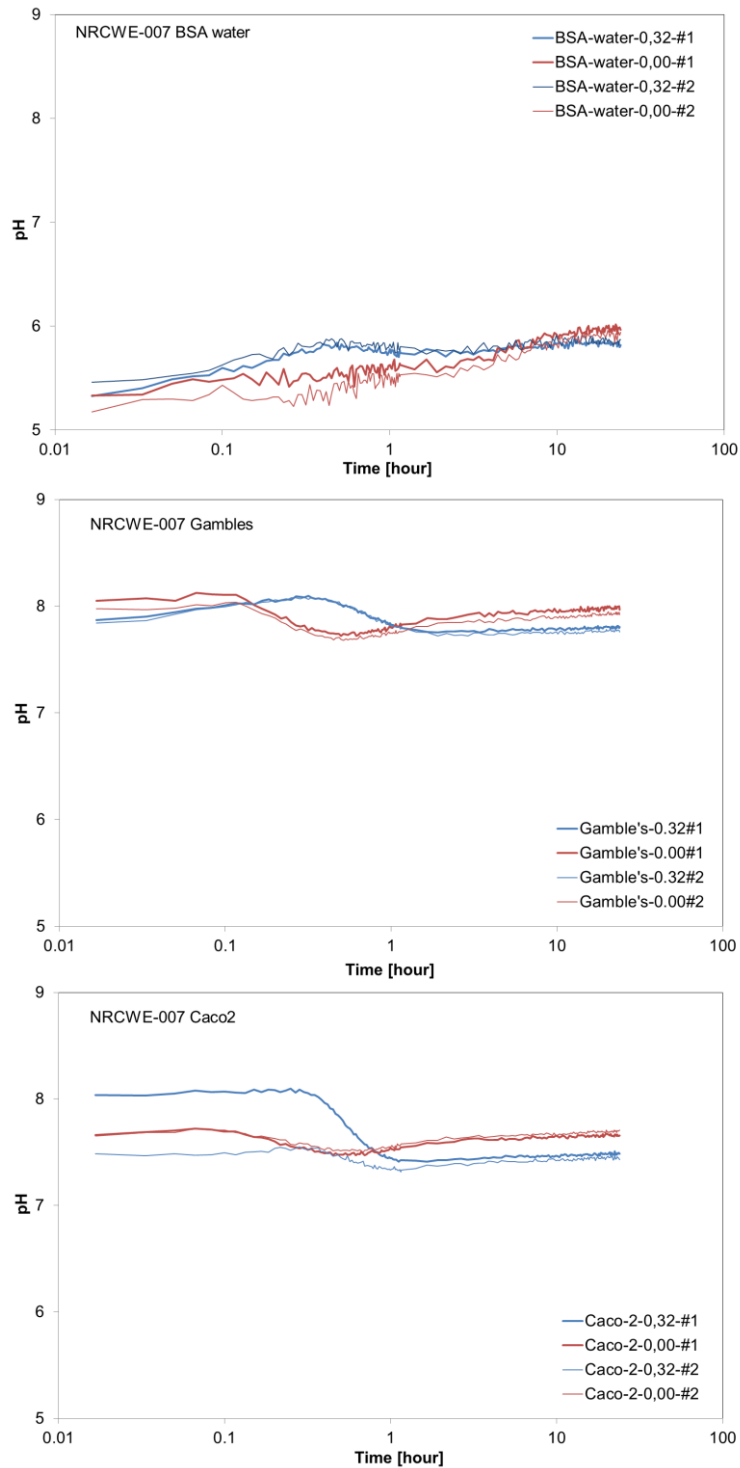
4.2 Hydrochemical O₂ reactivity

Figures 4.15 to 4.30 show the temporal variation in dO_2 and shows that most of the MNs have minor to quite notable reactivity. Interestingly, the reactivity may not be exerted to similar degree in the different media. It appears as though the reactivity for the TiO_2 and SAS often is less pronounced in the BSA medium than in the Gambles solution and Caco 2 media. This may be to a lesser extent in the case of the MWCNT.

For TiO_2 MN, no notable reactivity was observed in BSA medium for NM103, NM104 and NM105. In addition NM104 and NM105 also showed low reactivity by slightly increased dO_2 in the other two test media. In Gambles solution and Caco 2 media, both NM-100 and NM-103 acted reductive by lowering the dO2 value. NM-102 caused increased dO_2 in these two media, whereas the dO_2 was only increased for NM-101 in Caco 2.

For SAS, increased dO_2 levels were, to some extent, observed in all three media for NM-200 (not Caco 2 medium), NM-201, NM-202, and NM-203, whereas NM204 is only slightly reactive.

For MWCNT, only NRCWE-006 was found to have negligible dO_2 reactivity. Limited reactivity was also found in all BSA water dispersions, where only NM-402 and NRCWE-007 was able to induce significant increase in the oxygen level. As compared to all TiO2 and SAS MN's it is noteworthy that MWCNT did not cause clear negative dO_2 values suggesting that all MWCNT reactions result in net O_2 release of electron consumption.

For all MN samples, the maximum dO_2 change is on the order of 40 µmol/ml. Considering the applied doses, this suggest that the particle reactivity easily can exceed 1 µmol O_2/mg.

4.3 In vitro dissolution and solubility

Table 4.1 present the elemental analysis of the carefully prepared particle-free media, which show that the three media give only minor background concentrations of Ti, Si, Al, and Fe, Co, and Ni, which were the key target elements for assessing the 24-hour MN dissolution ratios (Table 4.2).

Table 4.1. Elemental concentrations in concentrations in the investigated incubation media (n=6)

MDL€	Element	unit	BSA	σ	Gambles	σ	Caco2	σ
1	K		<	<	<	<	160	<
1	Si	mg/l	<	<	<	<	<	<
0.05	Fe		<	<	<	<	0.31	0.36
30	Al		<	<	<	<	<	<
5	Ti		7.6	1.0	10.2	1.4	11.5	1.3
1	Cr		0.9	0.7	1.3	0.4	1.8	0.6
5	Co	µg/l	<	<	<	<	<	<
1	Ni		1.8	0.8	1.97	0.33	2.4	1.5
5	Zn		22.3	11.5	11.0	3.8	88	7

€ MDL = Minimum detection limit ; < = not detected or below MDL.

*Figure 4.15. O$_2$-evolution during 24-hour incubation of NM-100 in **a)** 0.05% BSA water NANOGENOTOX batch dispersion; **b)** Gambles solution; and **c)** Caco2 cell medium. The particle concentrations in the Gambles solution and Caco2 cell medium were dosed from the batch dispersion tested in a).*

*Figure 4.16. O_2-evolution during 24-hour incubation of NM-101 in **a)** 0.05% BSA water NANOGENOTOX batch dispersion; **b)** Gambles solution; and **c)** Caco2 cell medium. The particle concentrations in the Gambles solution and Caco2 cell medium were dosed from the batch dispersion tested in a).*

*Figure 4.17. O$_2$-evolution during 24-hour incubation of NM-102 in **a)** 0.05% BSA water NANOGENOTOX batch dispersion; **b)** Gambles solution; and **c)** Caco2 cell medium. The particle concentrations in the Gambles solution and Caco2 cell medium were dosed from the batch dispersion tested in a).*
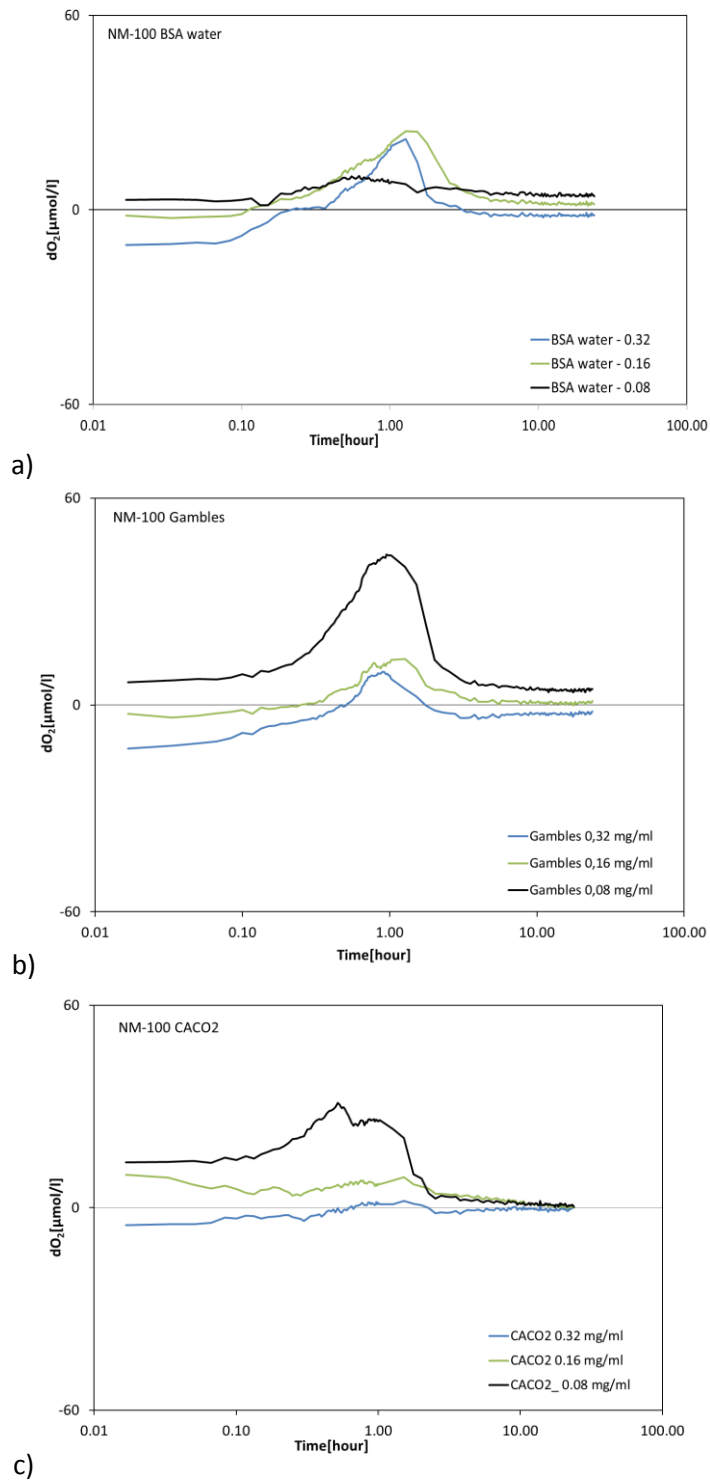
Figure 4.18. O₂-evolution during 24-hour incubation of NM-103 in **a)** 0.05% BSA water NANOGENOTOX batch dispersion; **b)** Gambles solution; and **c)** Caco2 cell medium. The particle concentrations in the Gambles solution and Caco2 cell medium were dosed from the batch dispersion tested in a).

33

a)

b)

c)

*Figure 4.19. O₂-evolution during 24-hour incubation of NM-104 in **a)** 0.05% BSA water NANOGENOTOX batch dispersion; **b)** Gambles solution; and **c)** Caco2 cell medium. The particle concentrations in the Gambles solution and Caco2 cell medium were dosed from the batch dispersion tested in a).*
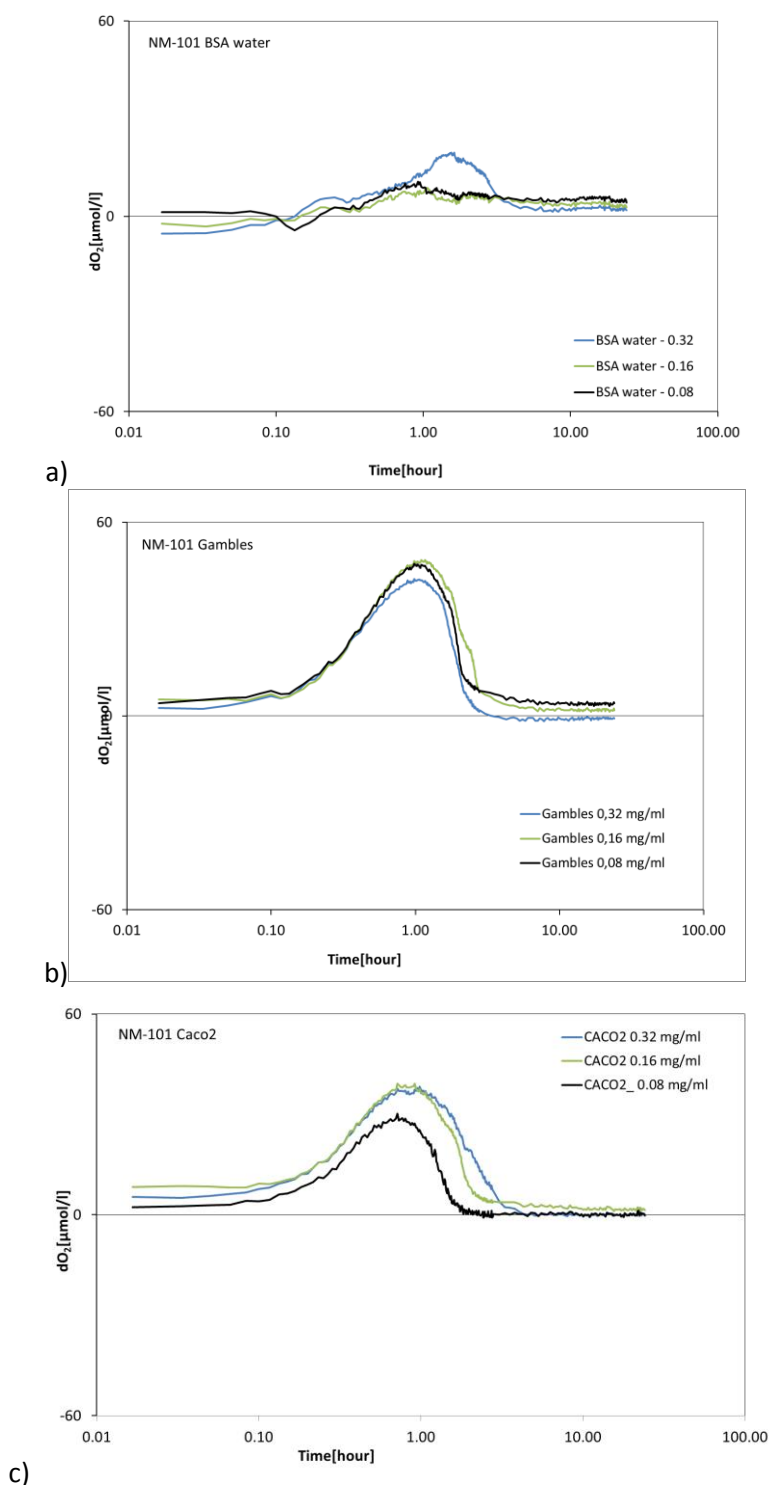
*Figure 4.20. O₂-evolution during 24-hour incubation of NM-105 in **a)** 0.05% BSA water NANOGENOTOX batch dispersion; **b)** Gambles solution; and **c)** Caco2 cell medium. The particle concentrations in the Gambles solution and Caco2 cell medium were dosed from the batch dispersion tested in a).*

Figure 4.21. O_2-evolution during 24-hour incubation of NM-200 in **a)** 0.05% BSA water NANOGENOTOX batch dispersion; **b)** Gambles solution; and **c)** Caco2 cell medium. The particle concentrations in the Gambles solution and Caco2 cell medium were dosed from the batch dispersion tested in a).
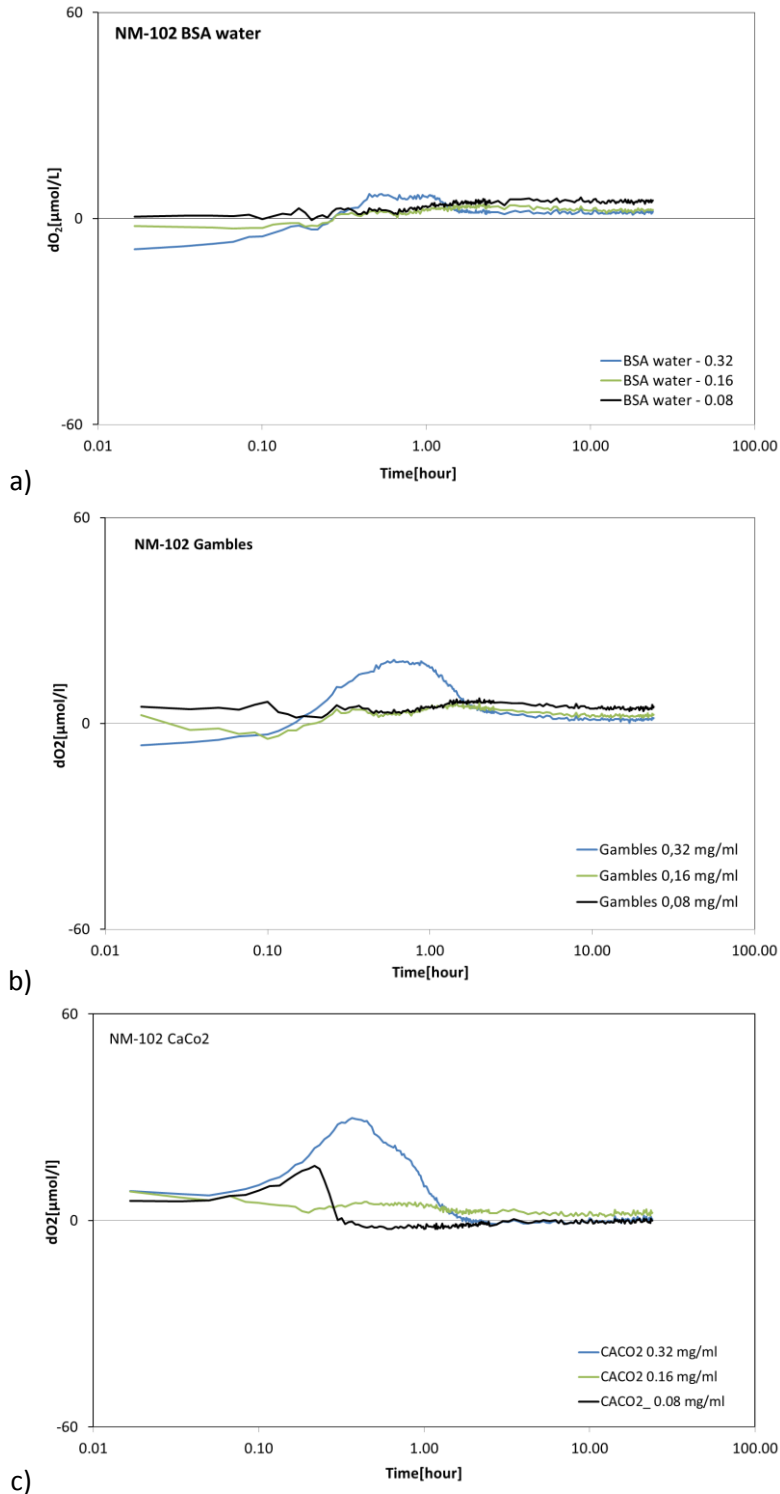
*Figure 4.22. O$_2$-evolution during 24-hour incubation of NM-201 in **a)** 0.05% BSA water NANOGENOTOX batch dispersion; **b)** Gambles solution; and **c)** Caco2 cell medium. The particle concentrations in the Gambles solution and Caco2 cell medium were dosed from the batch dispersion tested in a).*
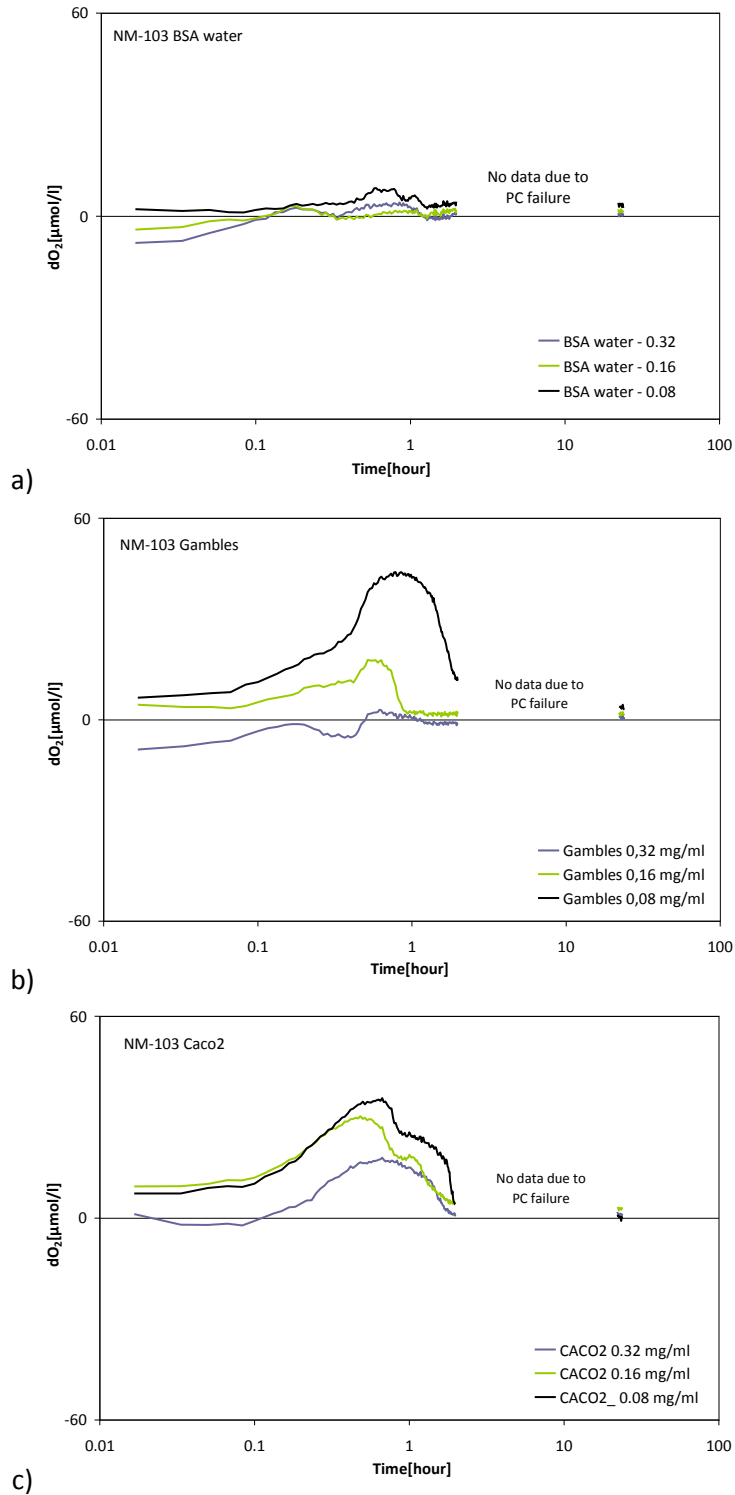
37
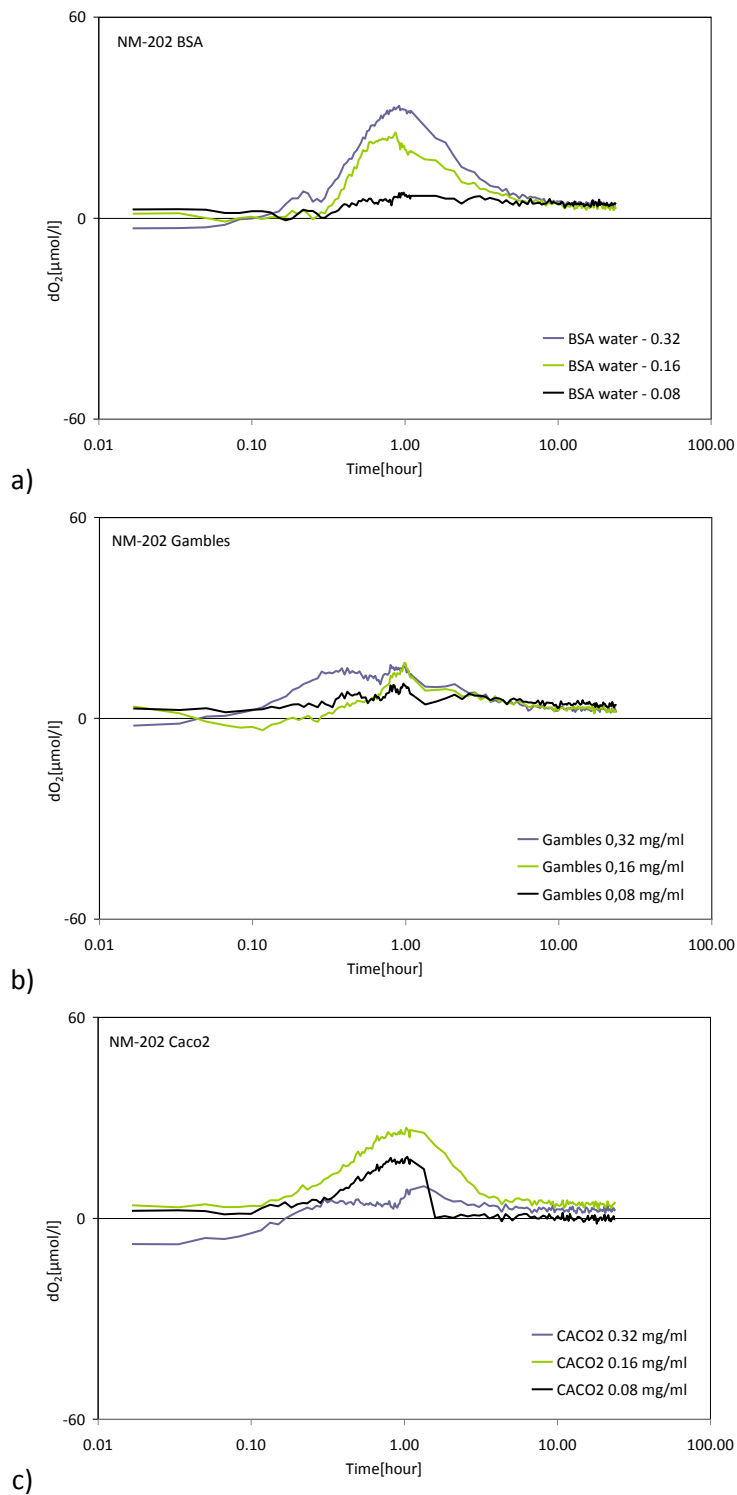
Figure 4.23. O$_2$-evolution during 24-hour incubation of NM-202 in a) 0.05% BSA water NANOGENOTOX batch dispersion; b) Gambles solution; and c) Caco2 cell medium. The particle concentrations in the Gambles solution and Caco2 cell medium were dosed from the batch dispersion tested in a).
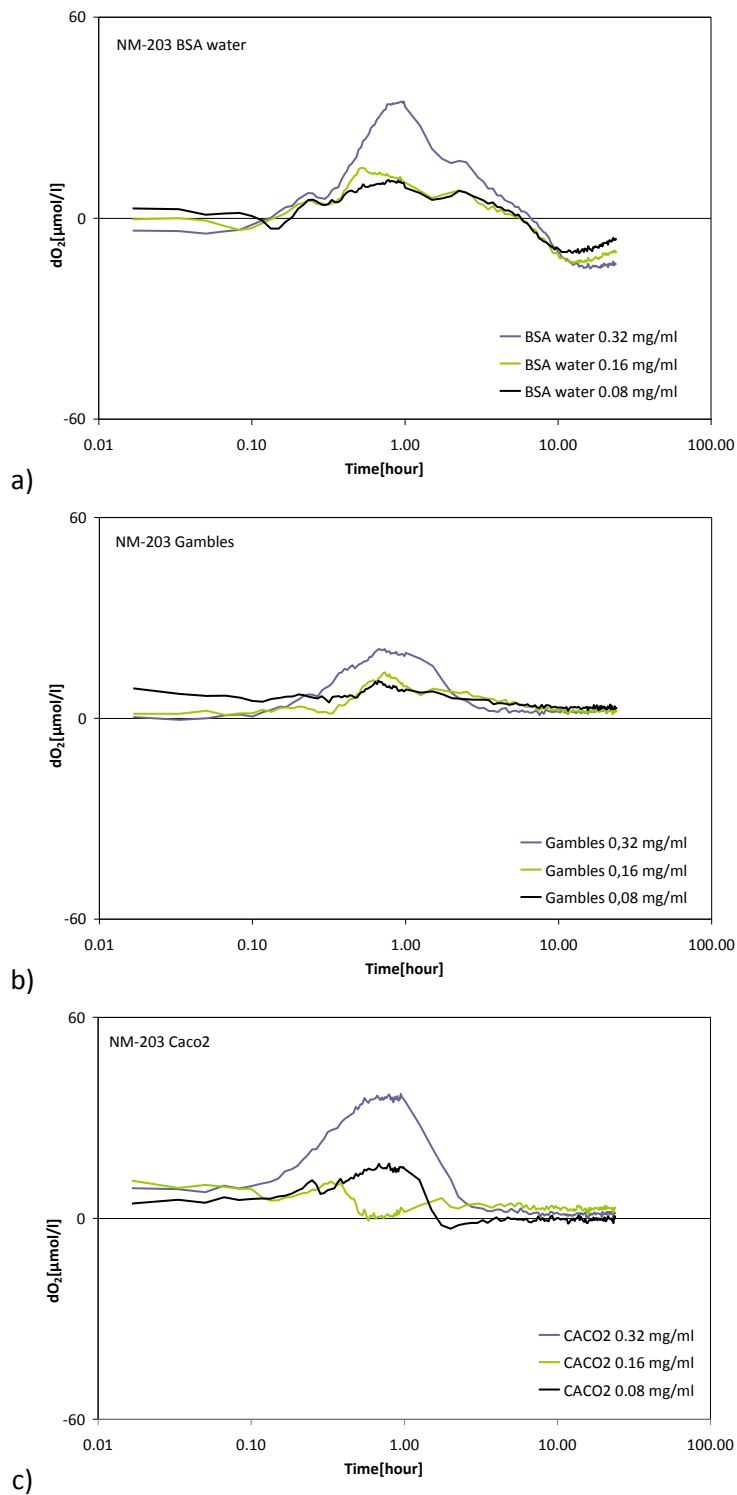
*Figure 4.24. O$_2$-evolution during 24-hour incubation of NM-203 in **a)** 0.05% BSA water NANOGENOTOX batch dispersion; **b)** Gambles solution; and **c)** Caco2 cell medium. The particle concentrations in the Gambles solution and Caco2 cell medium were dosed from the batch dispersion tested in a).*
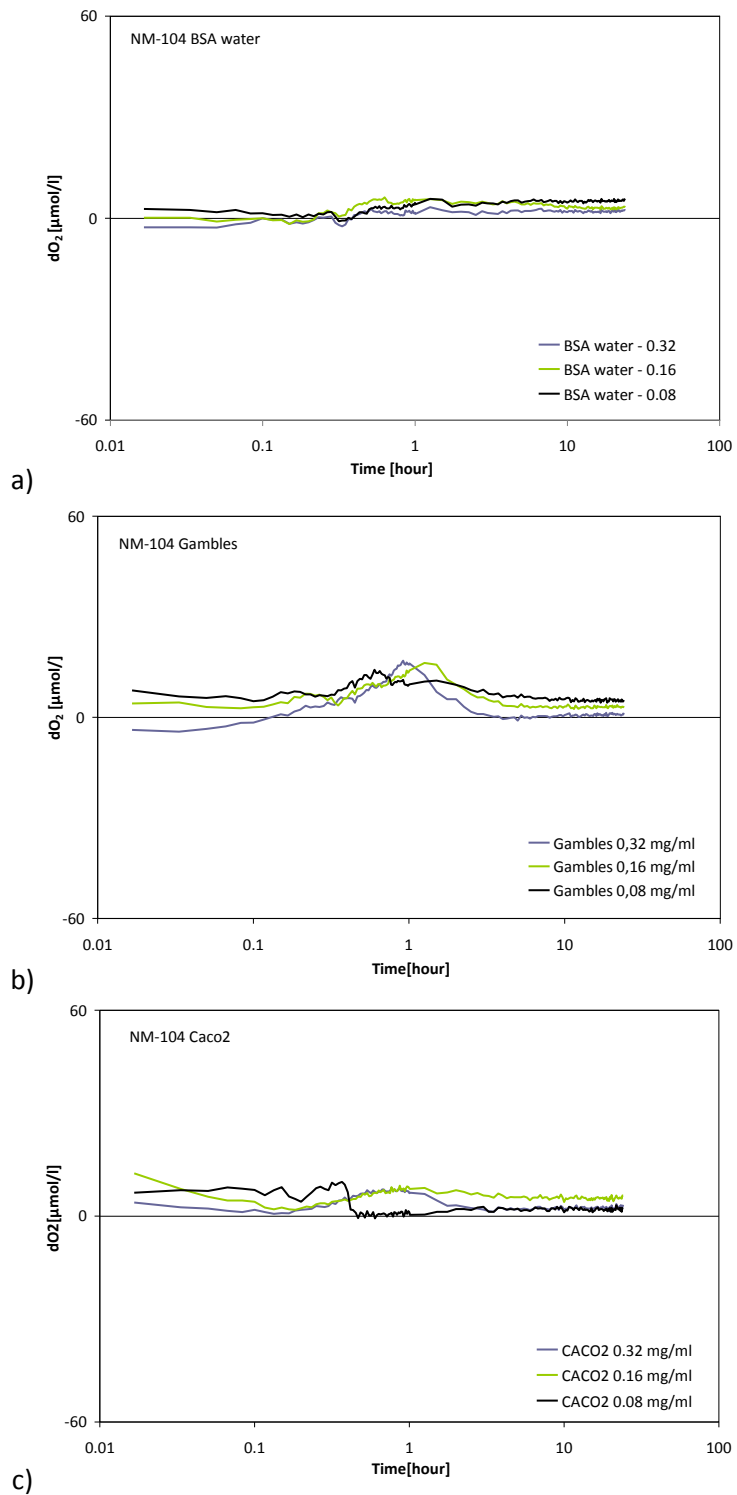
a)

b)

c)
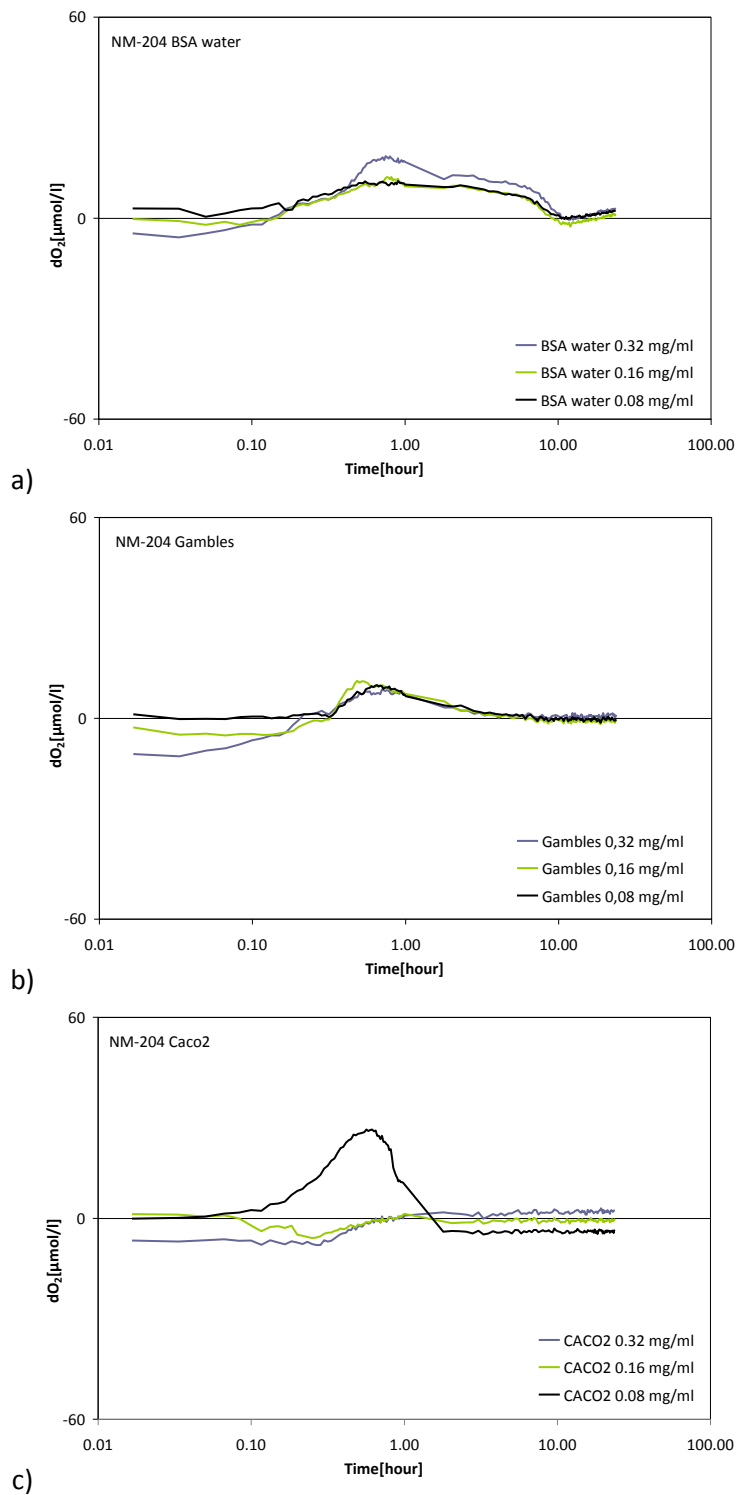
*Figure 4.25. O$_2$-evolution during 24-hour incubation of NM-204 in **a)** 0.05% BSA water NANOGENOTOX batch dispersion; **b)** Gambles solution; and **c)** Caco2 cell medium. The particle concentrations in the Gambles solution and Caco2 cell medium were dosed from the batch dispersion tested in a).*
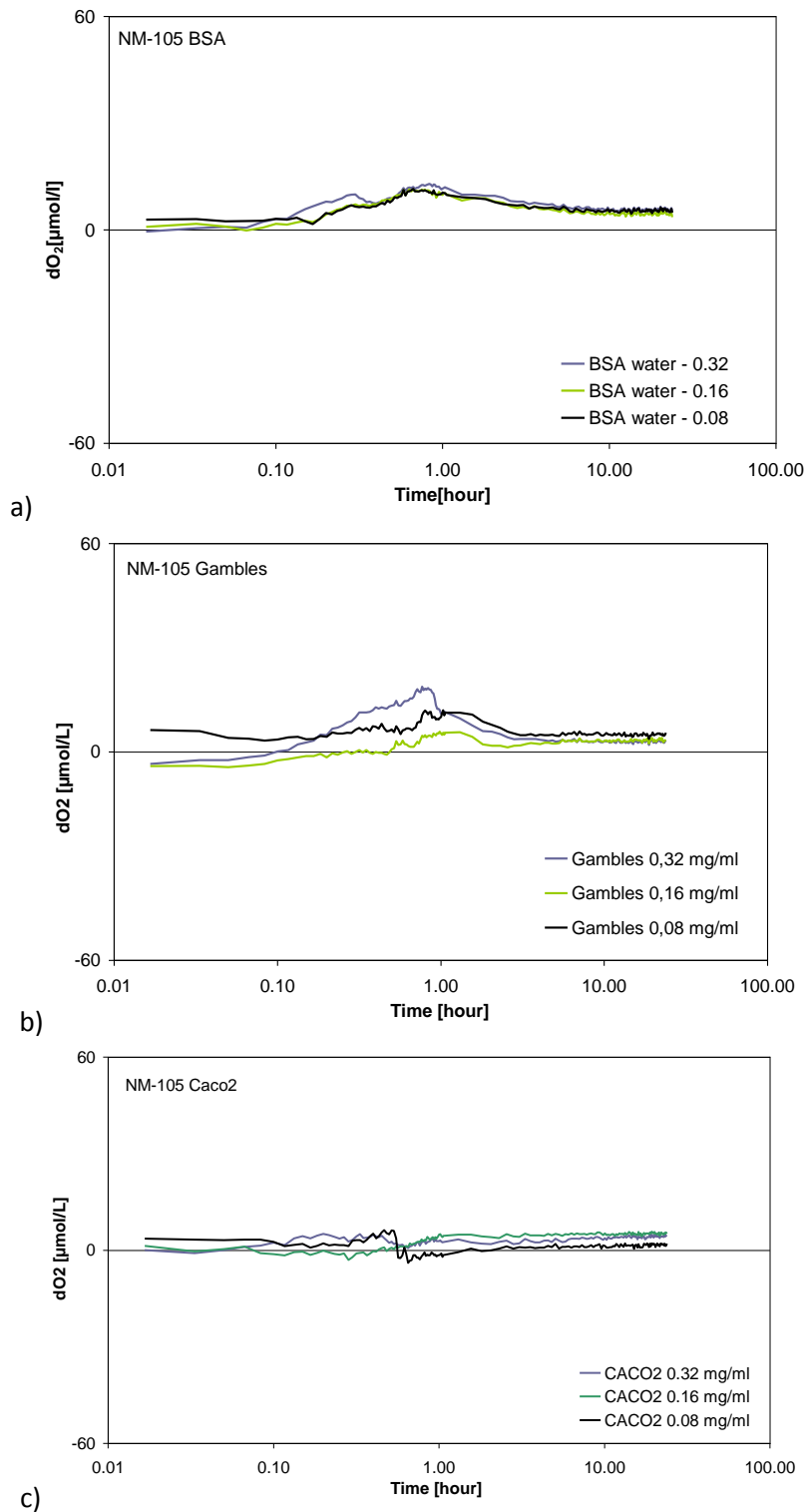
40

a)

b)

c)
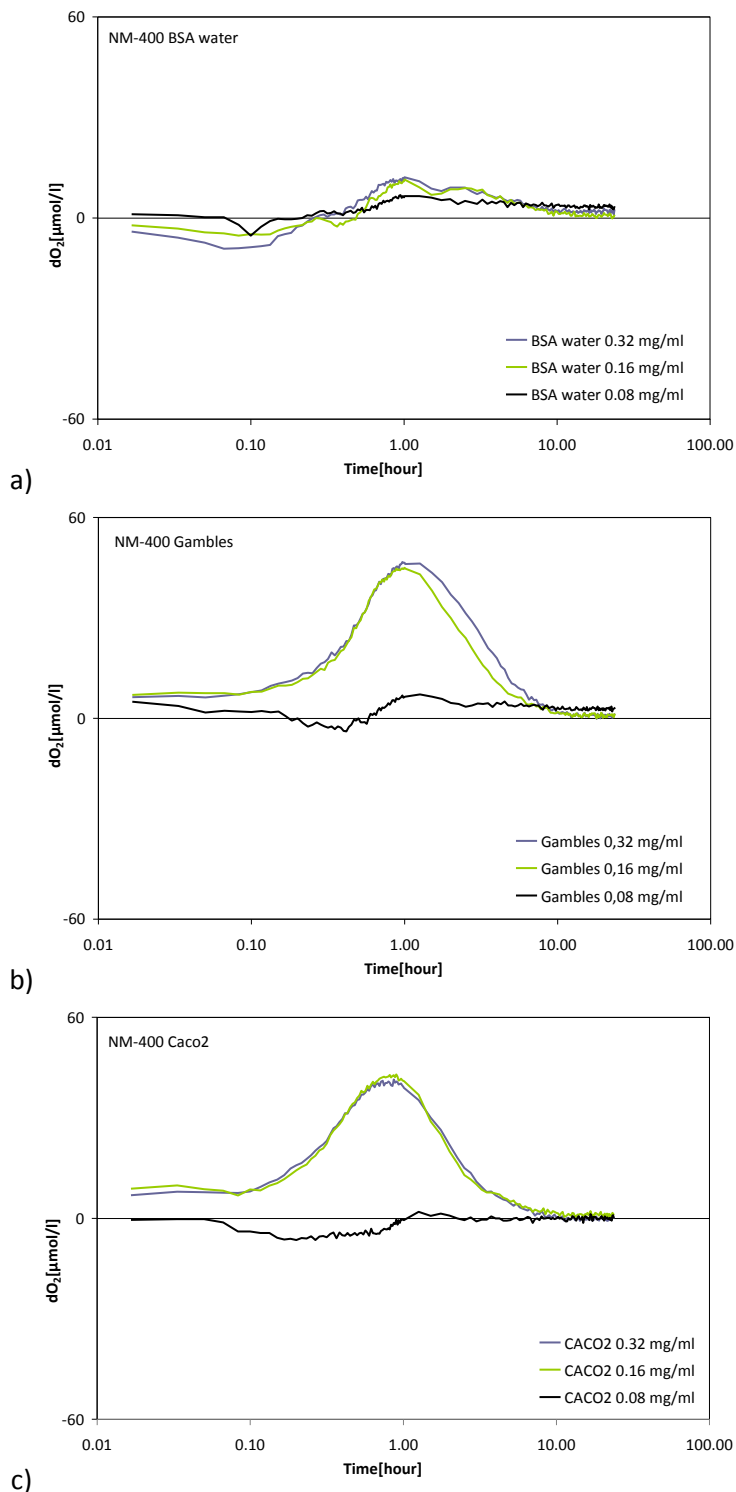
*Figure 4.26. O$_2$-evolution during 24-hour incubation of NM-400 in **a)** 0.05% BSA water NANOGENOTOX batch dispersion; **b)** Gambles solution; and **c)** Caco2 cell medium. The particle concentrations in the Gambles solution and Caco2 cell medium were dosed from the batch dispersion tested in a).*
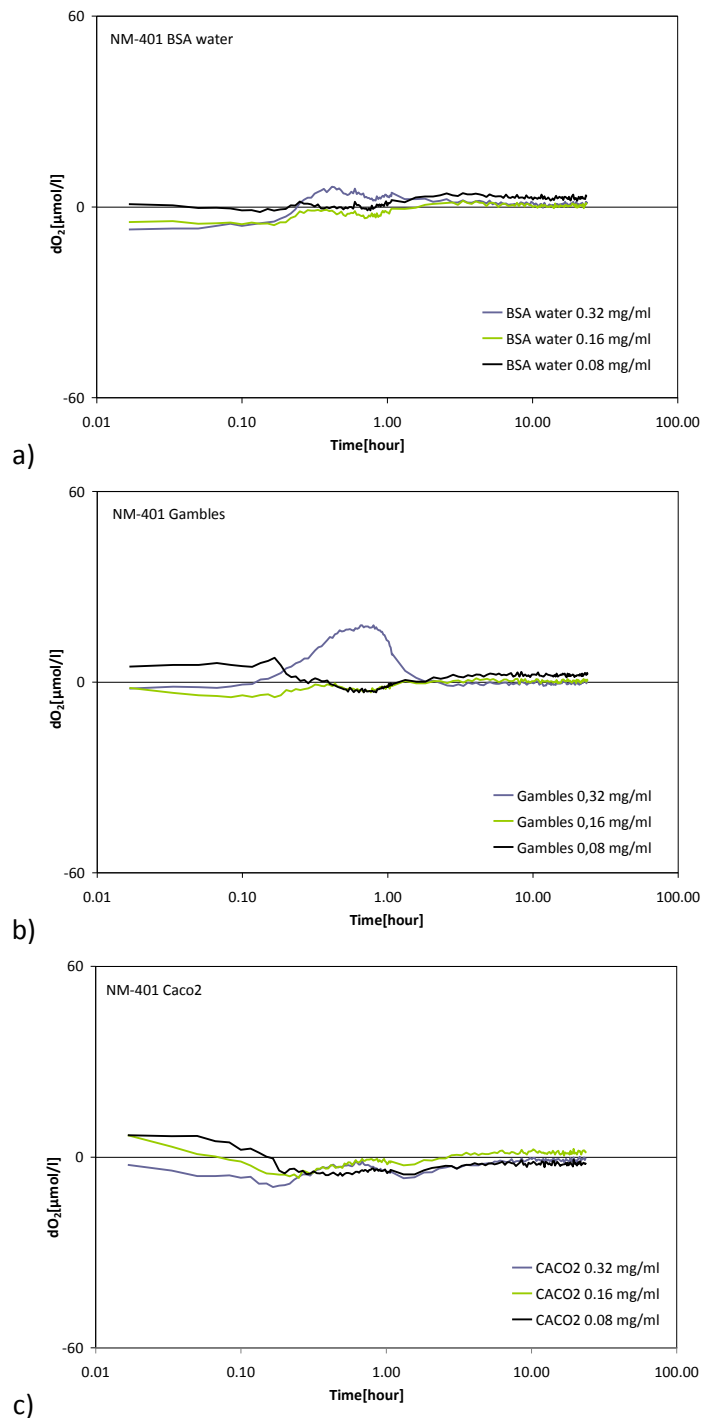
*Figure 4.27. O$_2$-evolution during 24-hour incubation of NM-401 in **a)** 0.05% BSA water NANOGENOTOX batch dispersion; **b)** Gambles solution; and **c)** Caco2 cell medium. The particle concentrations in the Gambles solution and Caco2 cell medium were dosed from the batch dispersion tested in a).*
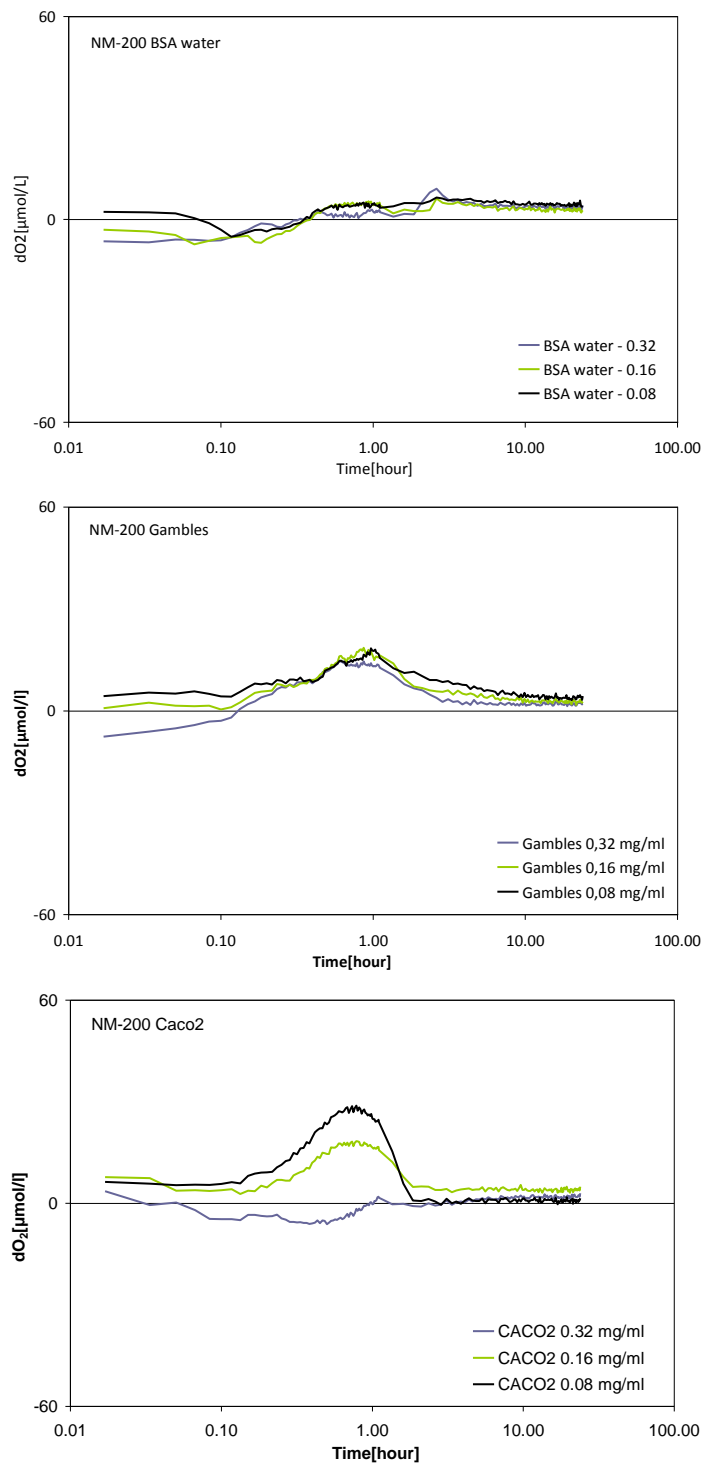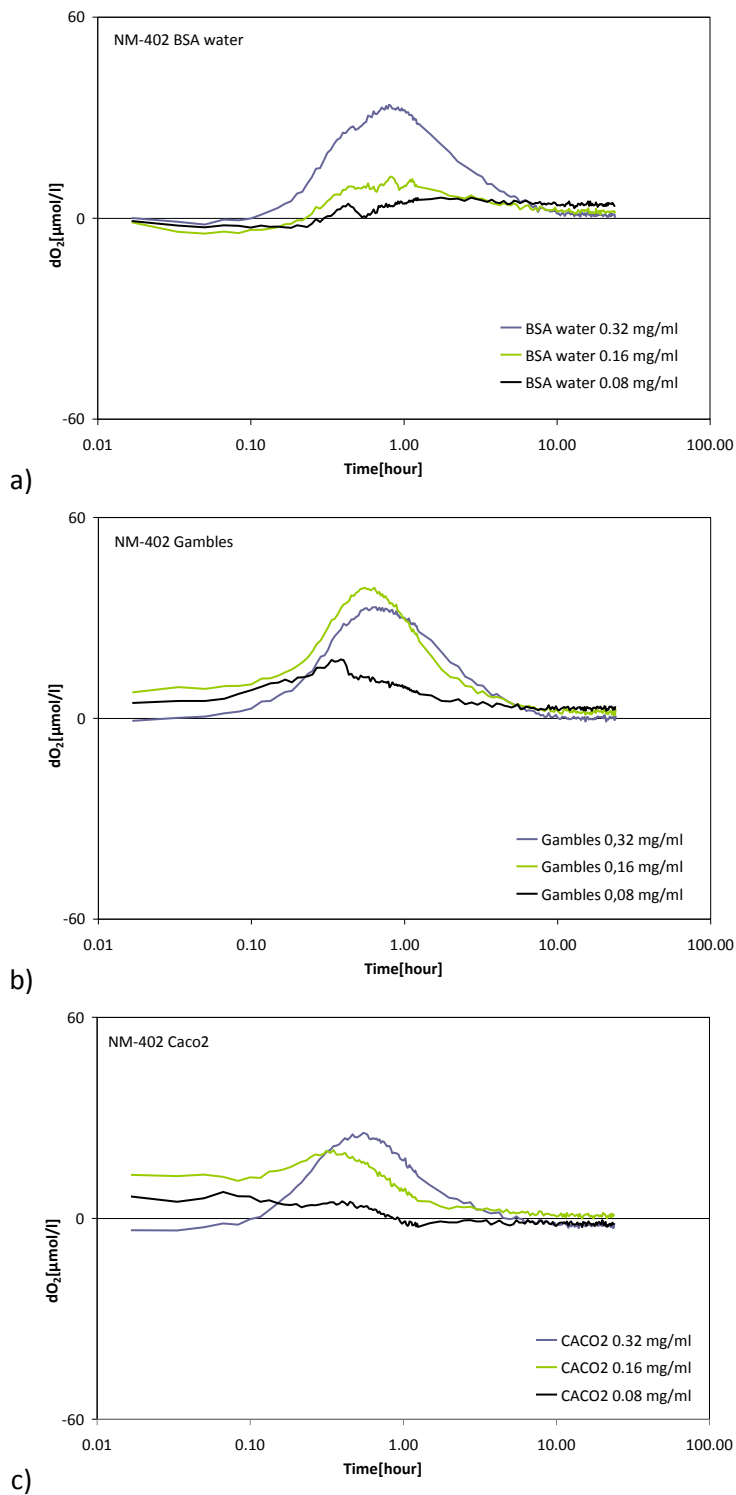
*Figure 4.28. O$_2$-evolution during 24-hour incubation of NM-402 in **a)** 0.05% BSA water NANOGENOTOX batch dispersion; **b)** Gambles solution; and **c)** Caco2 cell medium. The particle concentrations in the Gambles solution and Caco2 cell medium were dosed from the batch dispersion tested in a).*
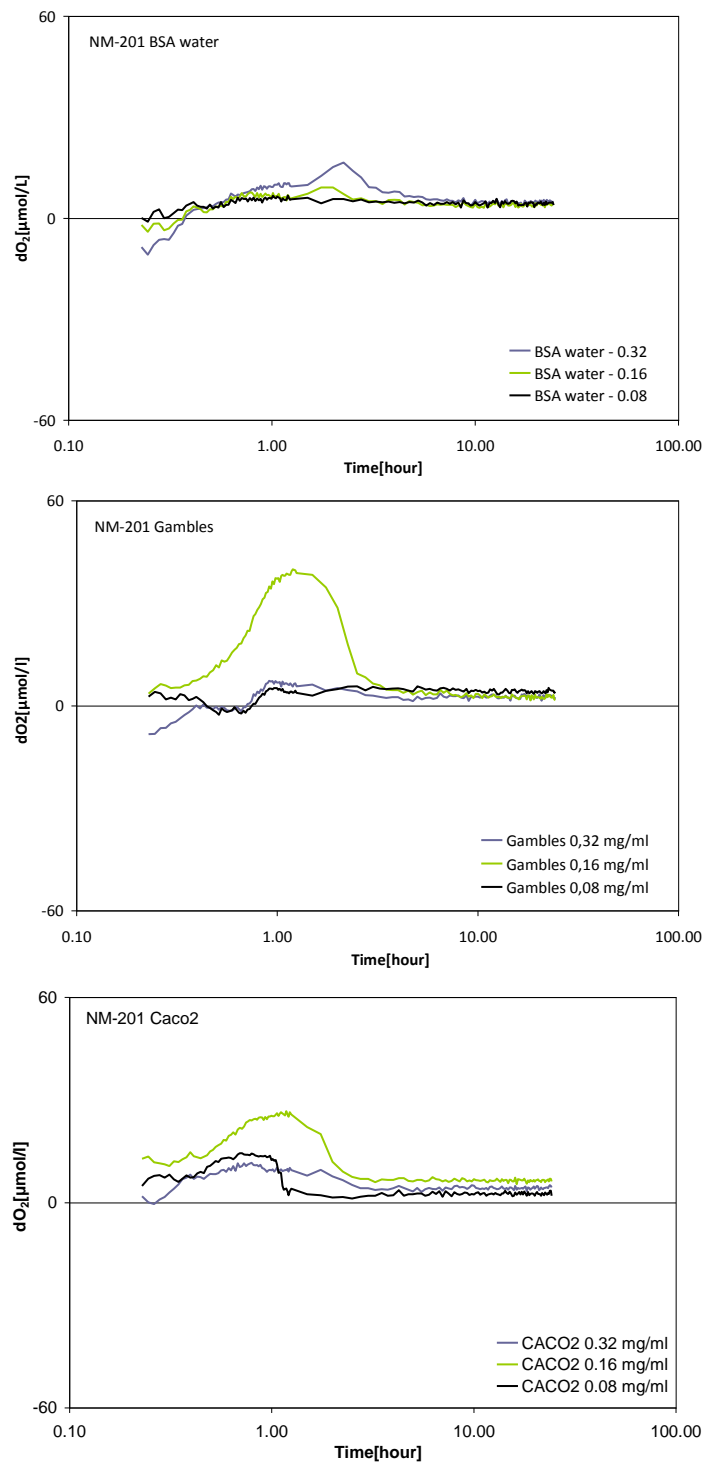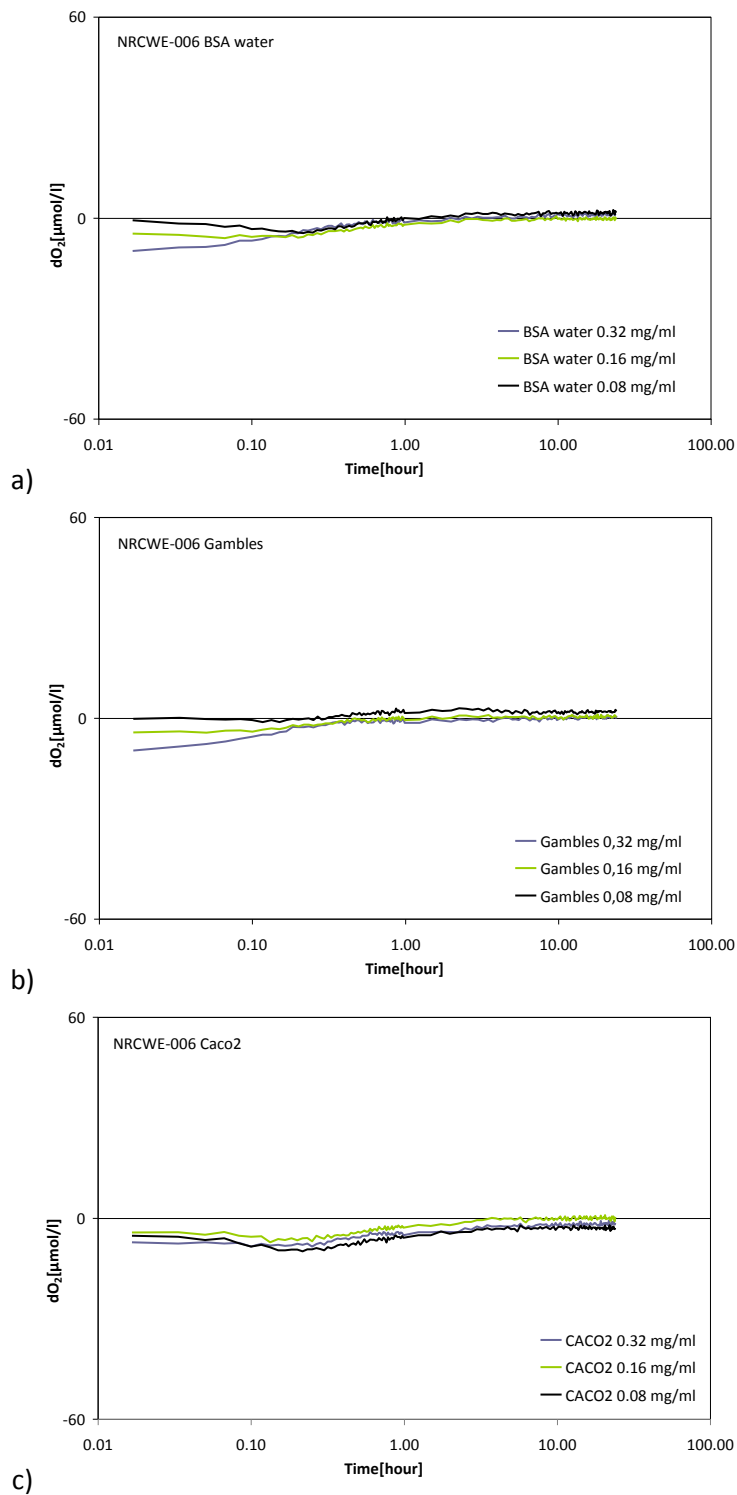
*Figure 4.29. O$_2$-evolution during 24-hour incubation of NRCWE-006 in **a)** 0.05% BSA water NANOGENOTOX batch dispersion; **b)** Gambles solution; and **c)** Caco2 cell medium. The particle concentrations in the Gambles solution and Caco2 cell medium were dosed from the batch dispersion tested in a).*

*Figure 4.30. O₂-evolution during 24-hour incubation of NRCWE-007 in **a)** 0.05% BSA water NANOGENOTOX batch dispersion; **b)** Gambles solution; and **c)** Caco2 cell medium. The particle concentrations in the Gambles solution and Caco2 cell medium were dosed from the batch dispersion tested in a).*
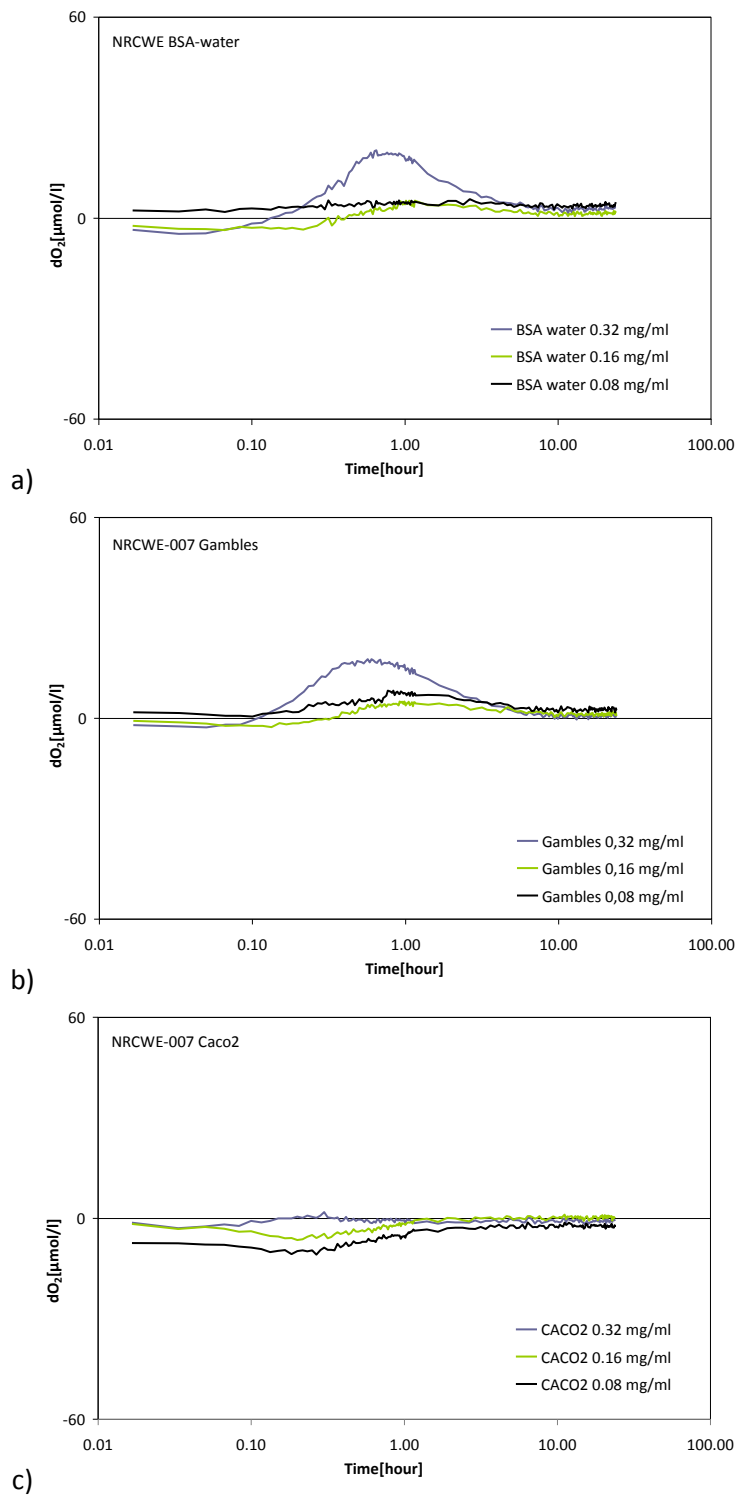
Table 4.2 list the elemental concentrations used for the assessment of MN solubilities and biodurability. Unfortunately, the consortium only made semiquantitative analyses on the TiO_2 and SAS MN and the quantitative ICP data made on the MWCNT MN are uncertain due to apparent incomplete extraction efficiencies as described in Deliverable 4.3 (Birkedal et al., 2012). Therefore, the assessment of 24-hour solubility limits and biodurable fraction must be considered approximate.

The compositions of the TiO_2 and SAS samples were obtained by IMC-BAS using energy dispersive spectrometry (EDS) on powder pellets in a scanning electron microscope (SEM) (Birkedal et al., 2012). The elements were verified by qualitative analyses were obtained by ICP-OES by CODA-CERVA. For MWCNT, the inductively coupled mass spectrometry (ICP-MS) data obtained from the collaborating partner, Duke University, were selected for the comparison. They were chosen as MWCNT data were the most complete and generally showed the highest concentrations (Birkedal et al., 2012). By that, it was inferred that the extraction procedure used by Duke University had highest yield and was closest to reality.

The TiO_2 MN samples have relevant high concentrations of Si, Al, Fe (NM-100, NM-102, and NM-103), and off-course Ti as the major element. Al is quite significant in the two surface treated samples. The SAS samples all contain Al in addition to Si. The MWCNT are the most complicated in this analysis and will be discussed based on their variable content of Al, Fe, Co, and Ni.

Table 4.2. Elemental concentrations (µg/g) in the MN samples used for assessment of dissolved fraction and particle biodurability.

Sample	Si	Al	Ti	Fe	Co	Ni
NM100	2,800	900	585,700	4,900	<	<
NM101	2,900	900	587,900		<	<
NM102	8,00	500	597,300	700	<	<
NM103	6,800	34,300	547,400	600	<	<
NM104	1,800	32,200	556,000	<	<	<
NM105	700	400	598,100	<	<	<
NM200	447,700	4,600	<	<	<	<
NM201	452,700	7,400	<	<	<	<
NM202	462,300	4,500	<	<	<	<
NM203	463,200	4,300	<	<	<	<
NM204	459,600	4,800	<	<	<	<
NM400	<	9,951±331	<	1,988±26	693±26	4±<
NM401	<	593±4	<	379±71	<	2±<
NM402	<	12,955±1530	<	16,321±664	2±<	9±1
NM403	<	2,024±168	<	7±4	2,881±190	58±4
NRCWE-006	<	66±19	<	355±2	<	1±<
NRCWE-007	<	86±24	<	480±13	116±21	4,843±289

< denotes values below 1 ppm or not detected /quantified

Tables 4.3 to 4.5 list the elemental compositions in the three incubation media corrected for the background concentrations in the incubation media. It is clear that most elements are present in relatively low concentrations. However, for proper assessment of the amount of dissolved matter, the calculation must be made using the applied elemental dose in the experiments. For this analysis, 0.32 mg/ml MN powder was dosed into each incubation media.

Table 4.3. Background-corrected elemental concentration in the test mediums after 24-hour dissolution tests with TiO$_2$ MN (n=2).

MDL			NM-100	σ	NM-101	σ	NM-102	σ	NM-103	σ	NM-104	σ	NM-105	σ
0.05% BSA														
1	mg/l	Si	-	-	-	-	-	-	0.9	1.3	-	-	-	-
30	µg/l	Al			175	49			198	116	137	25	-	-
5	µg/l	Ti	5.2	3.5	-	-	<	6.8	-	-	-	-	-	-
Gambles solution														
1	mg/l	Si	-	-	-	-	-	-	2.0	0.2	-	-	-	-
30	µg/l	Al	-	-	177	185	-	-	868	59	413	327	-	-
5	µg/l	Ti	-	-	-	-	3,388	3,900	-	-	-	-	-	-
Caco2													-	-
1	mg/l	Si	-	-	-	-	-	-	1.7	<	-	-	-	-
30	µg/l	Al	24	34	252	277	-	-	182	<	413	327	-	-
5	µg/l	Ti	796	2	3,414	1,683	1,741	683	222	337	3,386	3,900	2,724	3,846

MDL: Minimum detection limit in the raw analysis; - denotes not detected; < denotes background corrected concentration lower than 0.1 x MDL

47

Table 4.4. Background-corrected elemental concentration in the test mediums after 24-hour dissolution tests with SAS MN (n=2).

MDL			NM-200	σ	NM-201	σ	NM-202	σ	NM-203	σ	NM-204	σ	
0.05% BSA													
1	mg/l	Si	2.1	0.2	-	-	7.1	0.1	7.4	0.2	2.0	0.2	
30	µg/l	Al	105	16	231	148	145	92	90	6	84	55	
Gambles solution													
1	mg/l	Si	47.6	<	15.4	<	46.2	<	47.6	<	34.3	1.0	
30	µg/l	Al	71	8	178	65	73	12	238	79	-	-	
Caco2													
1	mg/l	Si	39.9	1.0	10.5	<	38.5	1.0	39.9	1.0	23.8	<	
30	µg/l	Al	301	10	217	30	72	3	104	43	224	40	

MDL: Minimum detection limit in the raw analysis; - denotes not detected; < denotes background corrected concentration lower than 0.1 x MDL

Table 4.5. Background-corrected elemental concentration in the test mediums after 24-hour dissolution tests with MWCNT (n=2).

MDL			NM-400	σ	NM-401	σ	NM-402	σ	NM-403	σ	NRCWE-006	σ	NRCWE-007	σ
0.05% BSA														
0.05	mg/l	Fe	0.23	0.05	-	-	-	-	-	-	0.11	0.03		
30	µg/l	Al	50	11	-	-	-	-	22	31	-	-	-	-
5	µg/l	Co	32	4	-	-	-	-	448	40	0.4	0.6	20	<
1	µg/l	Ni	3.8	2.1	<	1.1	<	1.1	8.4	1.4	23	3	138	1
Gambles solution														
0.05	mg/l	Fe	0.09	0.03	-	-	0.08	-	-	-	0.04	0.06	0.08	0.11
30	µg/l	Al	322	20	-	-	196	-	322	-	-	-	-	-
5	µg/l	Co	36	1	-	-	-	-	553	10	-	-	18	1
1	µg/l	Ni	6.3	7.0	0.3	0.6	<	0.5	10.6	0.5	0.5	1.0	151.2	0.5
Caco2														
0.05	mg/l	Fe	<	0.51	-	-	<	0.50	<	0.50	0.15	0.78	<	0.54
30	µg/l	Al	-	-	-	-	-	-	22	31	22	32	-	-
5	µg/l	Co	30.1	1.0	-	-	-	-	455	10	-	-	16.1	1.0
1	µg/l	Ni	2.7	4.3	<	2.2	<	2.2	8.0	2.3	<	2.3	136.6	2.2

MDL: Minimum detection limit in the raw analysis; - denotes not detected; < denotes background corrected concentration lower than $0.1 \times$ MDL

The elemental dose concentration was determined by simple multiplication of element concentration (Table 4.2) in µg/mg with the applied dose 0.32 mg sample/ml medium. These concentration data were used to calculate the weight percent of dissolved element using the background-corrected elemental concentrations in the three incubation media after 24-hour incubation (Tables 4.3 to 4.5). The results from these calculations are shown in Figures 4.31 to 4.33, for TiO_2, SAS and MWCNT, respectively.

The results from the dissolution studies with the TiO_2 MN show that that the TiO_2 as such are almost insoluble in all three media. When detected the values are on the order of 1 wt% of the 0.32 mg/ml dose used in the experiments. However, in contrast to the Ti, which is the key indicator of the principle MN, associated Si, Al, and Fe generally appear more soluble.
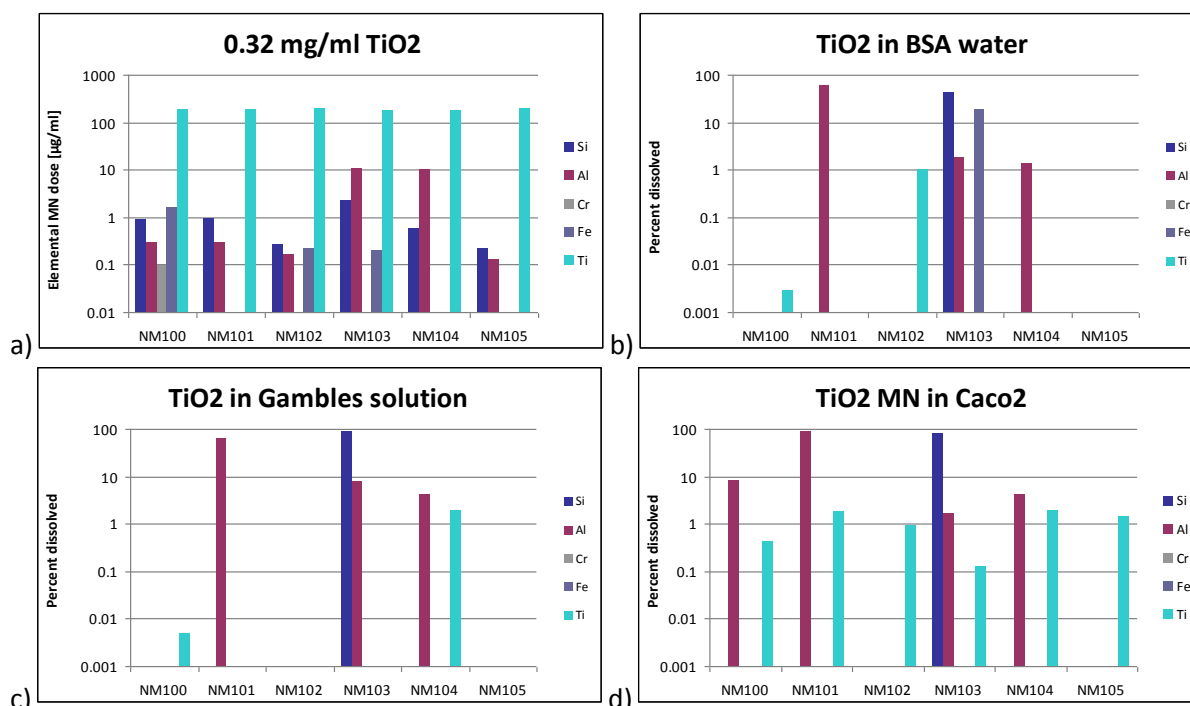

Figure 4.31. a) Elemental dose for most abundant elements in the TiO2 NM. b) Percent dissolved element in b) BSA water ; c) Gambles solution ; and d) Caco2 cell medium.

Al was indicated as coating material (EDS results indicated on the order of 3.2-3.4 wt%) in NM-103 and NM-104, but found as an trace element (0.04 to 0.09 wt%) in all semiquantitative EDS-analyses on the TiO_2 samples (Table 4.2). In the dissolution experiments, Al was observed in all three media incubated with NM-101, NM-103, and NM-104, as well as NM-100 incubated in Caco 2 cell medium. The amount of dissolved Al was on the order of 1-8 wt% in NM-103 and NM-104 with the highest Al contents. In the low-Al TiO2 samples, the fraction was up to 60-80 wt% (Figure 4.31).

EDS analysis indicated presence of Si (0.07 to 0.68 wt%) in all samples (Table 4.2). The highest concentrations were observed in NM-103, followed by NM-100, NM-101, and NM-104 (0.18-0.29 wt%). The Si concentration in NM-102 and NM-105 was in the order of 0.07-0.08. From the industry data, silicone (Dimethicone coating) was reported for NM-103 and NM-104. GC-MS analysis indicated presence of compounds tentatively identified as silanes in NM-101, NM-103, and NM-104, as well as possibly tetramethyl silicate in NM-104. Consequently, from the reported and project-generated knowledge about the test materials, Si is present in all TiO_2 samples and a fraction of the Si is present

50

as an organic compound in NM-101, NM-103, and NM-104. From dissolution studies, the elemental analyses only, but consistently, reveal presence of Si in experiments with NM-103 in all three incubation media. The fraction of dissolved Si varied between 42 (BSA-water) and 90 wt% (Gambles solution).

Fe was observed in three samples (NM-100, NM-102 and NM-103) by EDS (Table 4.2). The highest concentrations was found in NM-100 (0.49 wt%), whereas ca. 0.06 to 0.07 wt% was observed in NM-102 and NM-103. In the dissolution experiments, Fe was only detected in NM-103 incubated in BSA water. The fraction of dissolved Fe appeared to be on the order of 18 wt%.

Overall, the dissolution experiments with TiO_2 suggest, as would be expected, that only a very minor fraction of TiO_2 goes into dissolution. However, the Al and/ Si coating, or otherwise associated Al, Si, and Fe elements, appears more unstable and may at least partly dissolve during the 24-hour incubation experiment. For Si, part of the dissolved fraction may be explained by their presence as constituent elements in associated silane and silicone.

Figure 4.32 shows the elemental dose and the percent dissolved Si and Al in the three incubation media from the dissolution experiments with SAS. Naturally the elemental dose is heavily dominated by Si, but the concentration of the Al impurities appear to be relevant as well. From the MN sample analyses, the highest Al-content was found in NM-201 (0.74 wt%) and it was on the order of 0.4 to 0.5 in all the other SAS samples (Table 4.2; Figure 4.32). The presence of Al is, at least in some samples, due to associated boehmite found by XRD in NM-200, NM-201, NM-202, and NM-203 (Birkedal et al., 2012). But from the XRD analyses, it cannot be excluded to occur also in NM-204.
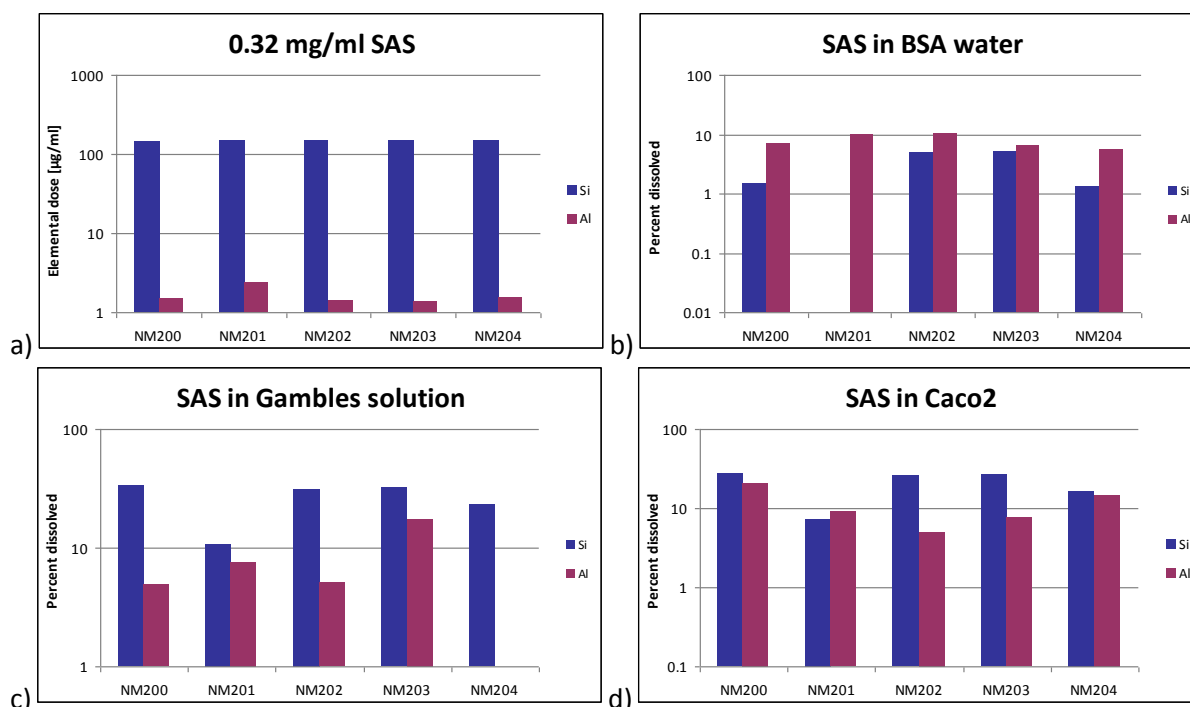

Figure 4.32. a) Elemental dose for most abundant elements in the SAS NM. b) Percent dissolved element in b) BSA water; c) Gambles solution; and d) Caco 2 cell medium.

From Figure 4.32, it is observed that the fraction of dissolved impurity Al (phase) and the fraction of dissolved Si, does rarely match completely. This suggests different behaviour of the SAS and Al

51

impurity (phase). In BSA-water, the fraction of dissolved Al exceed the fraction of dissolved Si, but this relationship is opposite in Gambles solution and the Caco 2 media. The amount of dissolved Al varies from 7.8 to 10.5 wt% in the BSA-water, <MDL to 17 wt% in Gambles solution, and 5 to 20 wt% in Caco 2 cell medium (Figure 4.32). Si was not detected for NM-201 in BSA and Al was not detected for NM-400 in Caco 2 cell medium. Note that the most reliable Al dissolution data are probably from the relatively high concentrations in NM-201. Inferred from the Si-concentrations, the fraction of SAS vary from <MDL to 5 wt% in BSA-water, 10 to 33 wt% in Gambles solution, and 7 to 28 wt% in Caco 2 cell medium.

From the current dissolution data the SAS and associated Al-phase appears to be least soluble in the BSA water used for the generic batch dispersion protocol and that the SAS solubility in the Gambles solution may be slightly higher than in Caco 2 cell medium.

In the dissolution experiments with MWCNT, the actual degradation of MWCNT cannot be assessed from pure elemental analyses. It is assumed that the tubular and graphite carbon material in the MWCNT samples are non- degradable at the applied test conditions. However, the catalyst and impurity materials identified by elemental analysis and electron microscopy (De-Temmerman et al., 2012; Birkedal et al., 2012) may behave differently. In this study, Al, Co, Fe and Ni were used as indicators for the catalyst dissolution. Following similar calculations as above, Figure 4.33 shows the dose concentrations and the percent dissolved element in the three incubation media. It is evident that Al and/or Fe are the major impurities in all samples, except from NRCWE-007, where Ni is the most abundant impurity. The measured concentrations of Al and Fe do reach percent levels in NM-400 (1.0 wt% Al; 0.2 wt% Fe) and NM-402 (1.3 wt% Al; 1.6 wt% Fe). Ni reach 0.48 wt% in NRCWE-007.
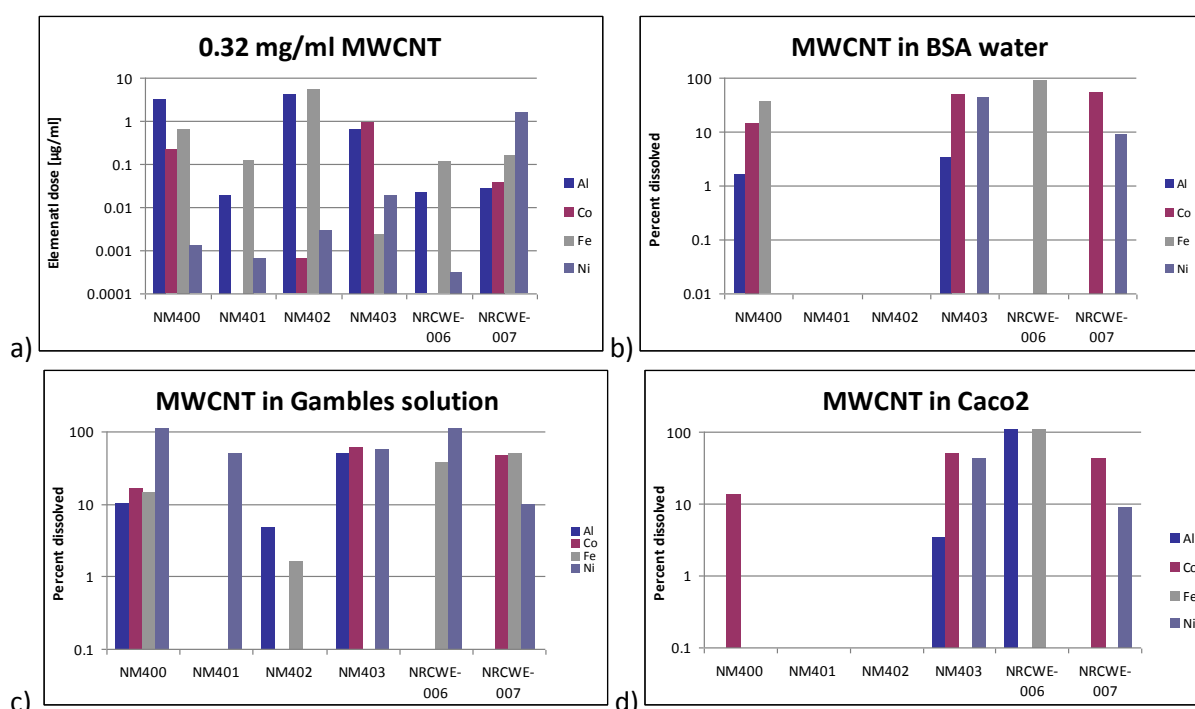

Figure 4.33. a) Elemental dose for most abundant elements in the MWCNT NM. Percent dissolved element in b) BSA water; c) Gambles solution; and d) Caco2 cell medium.

Due to the relatively low measured elemental concentrations in the MWCNT, the most reliable data are to be expected for Al and Fe in NM-400 and NM-402, Al and Co in NM-403, and Ni in NRCWE-007 (Table 4.2; Figure 4.33). The concentrations of the four selected elements may be too low in NM-401 (≤ 0.06 wt%) and NRCWE-006 (≤ 0.04 wt%) for reliable assessment even by ICP-OES (Table 4.2; Figure 4.33). However, the data are still kept for indication, because some of the elements were sometimes detected in the test media after the 24-hour dissolution test.

The results from the analyses, suggest slightly different behavior of the catalyst materials in the three different incubation media. For NM-401 and NM-402, no dissolution was detected in BSA water and Caco 2 cell medium (Figures 4.33b and d). Some degree of dissolution was observed for all other samples and media combinations. Considering first elements with relatively high concentrations, it was found that:

NM-400
Al was found to partially dissolve in BSA-water (1.6 wt%) and Gambles solution (10.1 wt%)
Fe was found to partially dissolve in BSA-water (36.3 wt%) and Gambles solution (14.3 wt%)
Co was found to partially dissolve in all three media: BSA-water(36.3 wt%), Gambles solution (14.3 wt%) and Caco 2 cell medium (13.6 wt%).

NM-402:
Al was found to partially dissolve in Gambles solution (4.7 wt%)
Fe was found to partially dissolve Gambles solution (1.6 wt%)

NM-403:
Al was found to partially dissolve in all three media: BSA-water (3.4 wt%) and Gambles solution (49.7 wt%), and Caco 2 cell medium (3.4 wt%).
Co was found to partially dissolve in all three media: BSA-water (48.6 wt%), Gambles solution (60 wt%) and Caco 2 cell medium (49.4 wt% wt%).

NRCWE-007:
Ni was found to partially dissolve in all three media: BSA-water (8.9 wt%), Gambles solution (9.8 wt%) and Caco 2 cell medium (8.8 wt% wt%).

For very low concentration elements in the MWCNT, higher percentages of dissolution was often found. For example, a high fraction of Ni (51 wt%) was found to be dissolved in the test of NM-401 and for NM-402 (Figure 4.33c). Sometimes, the dissolved Ni fraction even exceeded 100% (NM-400 and NRCWE-006). The fraction of dissolved Co was also relatively high in all test media (13.6 to 60 wt%). For these two elements, the observed high dissolved fractions may be due to MWCNT elemental concentrations too low for quantification, sample inhomogeneities, or too low yield in the elemental analyses on the powders. The samples are indeed known to be inhomogeneous and low elemental quantification yield of the MWCNT has also been indicated (Birkedal et al., 2012). Therefore, the dissolution data on especially the low concentration impurities in the MWCNT should only be considered indicative.

4.4 Estimation of biodurability

The results from the 24-hour reactivity and dissolution tests can give some indication on the biodurability of the test materials. It is interesting to note that the elemental analysis have shown different behavior of the different elements. In TiO$_2$, minor elements were present due to inorganic

53

and organic coatings. In SAS, Al was present due to impurity phases of boehmite. MWCNT contained several different impurity elements due to Al and different transition metal catalyst particles.

From the analyses, we can conclude that all TiO_2 samples are categorized as higly durable nanomaterials. However, their coatings may degrade rapidly over the first 24-hours. The degradation appears to vary with the three incubation media used and was most pronounced in the Caco 2 cell medium.

The SAS and associated boehmite was, with a few exceptions, partially dissolved in all incubation media. Based on measured Si-concentrations, the average 24-hour SAS dissolution is about 3.2 wt% in BSA water and 20 to 26 wt%. On average 8 and 11 wt% of the associated Al is dissolved in three different media. Based on these observations, it is concluded that the SAS MN have moderate biodurability in lung lining fluids and the intestine. The apparently higher biodurability in the BSA-water, is advantageous from experimental points of view, because less SAS is expected to degrade before onswet of actual exposure.

For MWCNT, it is assumed that the carbon structure is not degradable in the three incubation media and the given test conditions. However, the associated catalyst impurities appear to dissolve, at least partially, during the 24-hour reactivity and dissolution test. For the elements with relatively high abundance, the dissolved fraction did not exceed 50 wt%. For Al (good tracer for NM-400; NM402; and NM-403), up to 3.4 wt% was observed to dissolve in BSA water, 4.7 to 49.7 wt% were dissolved in Gambles solution and up to 3.4 wt% were dissolved in Caco 2 medium. For Fe (good tracer for NM-400 and NM-402), 0 to 36 wt% were dissolved in BSA-water, 1.6 to 14.3 wt% was dissolved in Gambles solution, and nothing was dissolved in Caco 2 cell medium. For Co (good tracer for NM-403) 48.6 wt% was dissolved in BSA-water, 60 wt% was dissolved in Gambles solution, and 49.9 wt% was dissolved in Caco 2 cell medium. Finally for Ni (good tracer for NRCWE-007), 8.9 wt% was dissolved in BSA-water, 9.8 wt% was dissolved in Gambles solution, and 8.8 wt% was dissolved in Caco 2 cell medium. Consequently, the biodurability of the catalyst materials appears to be high to moderate and, remembering that these analyses are made on minor and trace elements, appear to vary considerably between samples and media. This suggests that the speciation of the individual impurity elements may not be the same across all samples.

Conclusions

A screening method for assessment of the 24-hour hydrochemical pH and O_2 (proxy for redox) reactivity and solubility was established for pH 5 to 9 and O_2 saturation levels from 0 to 250% (0 to 707.6 µmol O_2/L). Temperature and atmospheric conditions (37°C; 5% CO_2, 95% RH) is maintained by a cell incubator. Tests were completed on 6 TiO_2 samples, 5 SAS samples, and 6 MWCNT samples.

pH reactivity tests revealed negligible to moderate effects on pH of the tested MN in 0.05% w/v BSA-water, Gambles solution, and Caco 2 cell medium. However, relatively great variations could occur during the course of the experiment, which are tentatively assumed to be due to small fluctuations in CO_2 concentrations delivered from external pressure tanks.

O_2 reactivity tests showed negligible to relatively high material and media-dependent effects on dO_2 (difference between O_2 concentration in dosed and reference vials).

- For TiO_2 MN no dO_2 reactivity was observed in BSA-water and NM-104 and NM-105 had also no to very low reactivity in Gambles solution and Caco 2 cell medium. NM-100 and NM-103 lowered dO_2 in Gambles solution and Caco 2, whereas NM-102 increased dO_2 in these two media. NM-102 only caused dO_2 increase in the Caco 2 medium.
- For SAS MN, increased dO_2 values were observed in all test media for NM-200 (not Caco 2 medium), NM-201, NM-202, NM-203, whereas a slight reduction was observed with NM-204.
- For the MWCNT, only NRCWE-006 had negligible dO_2 reactivity. All other samples generally caused increased dO_2 values. Yet, NM-402 and NRCWE-007 were the only samples to notably increase dO_2 values in BSA-water.

Evaluation of MN dissolution and biodurability revealed different material-depending behavior. The variation was partially linked to presence of coatings in TiO_2, presence of associated impurity phases in SAS, and presence of different catalyst particles and substrates in the MWCNT samples.

- TiO_2 has very low solubility, but a high fraction of the Al and Si coating appears to be partly or completely released to the media in the 24-hour experiment. Highest dissolution Consequently, the TiO_2 is durable, but the coatings may not be.
- SAS are partially dissolved in all three media. Si was not detected for NM-201 in incubation with BSA water and Al was not detected for NM-204 incubated in Gambles solution. The relative fraction of dissolved Si (average = 3 wt%) is lower than for Al (average = 8 wt%) in BSA-water, but similar (average 21 to 26 wt%) or higher than for Al in Gambles solution (9 wt%) and Caco 2 cell medium (11 wt%). Consequently, SAS and the associated Al, of which some is present as boehmite, is considered to have moderate biodurability.
- The carbon materials in MWCNT are assumed to be highly durable in the selected incubation media and test conditions. However, the associated metal impurities and catalysts have moderate to high levels of dissolution. When the most abundant elements included Al and/or Fe, the dissolved fractions were often in the range of 1-15 wt%, but some were notably higher. For NM-401 and NM-402 (relative high concentrations of Fe and Al + Fe, repectively), no dissolution was observed in BSA-water and Caco 2 cell medium. In samples with Co, 13-16 wt% (NM-401) to 43-60 wt% (NM-403, NRCWE-006 and NRCWE-007) was dissolved in all three media. In the Ni-rich sample (NRCWE-007) 8.8 to 9.8 wt% was dissolved in all three media. The dissolved fraction sometimes exceeded 100%. This may be due to sensitivity of very low concentration levels, inhomogeneity and potentially insufficient extraction of the metals in the analysis of the powder materials.

55

References

Birkedal R., Shivachev, B., Dimova L., Petrov O., Nikolova, R., Mast, J., De Temmerman, P.-J., Waegeneers, N., Delfosse, L., Van Steen, F., Pizzolan, J.C., De Temmerman, L., Deliverable 4.3: Crystallite size, mineralogical and chemical purity of NANOGENOTOX nanomaterials. Edited by Jensen K.A. and Thieret N., October 2012, 71 pp.

Christensen VR., Jensen SL., Guldberg M., Kamstrup O. (1995) Effects of chemical composition of man-made vitrous fibers on the rate of dissolution in vitro at different pHs. Environmental Health Perspectives 102/5, 83-86.

Cho, W.-S., Duffin, R., Howie, S.E.M., Scotton, C.J., Wallace W.A.H., MacNee, W., Bradley, M., Megson, I.L., Donaldson, K. (2011) Progressive severe lung injury by zinc oxide nanoparticles; the role of Zn2+ dissolution inside lysosomes. Particle and Fibre Toxicology 2011, 8:27

De-Temmerman, J., Mast, J., Guiot, C., Spalla, O., Rousset, D., Shivachev, B., and Tarrassov, M. Deliverable 4.2: Transmission electron microscopic characterization of NANOGENOTOX nanomaterials and comparison with atomic force microscopy. Edited by Jensen K.A. and Thieret N., October 2012, 71 pp.

Dick CAJ., Brown DM., Donaldson K., Stone V. (2003) The role of free radicals in the toxic and inflammatory effects of four different ultrafine particle types. Inhalation toxicology 15/1, 39-52

Jensen K.A., Kembouche, Y., Christiansen, E., N.R., Wallin, H., Guiot, C., Spalla, O., Witschger, O. Deliverable 3: Final protocol for producing suitable MN exposure media. Edited by Jensen K.A. and Thieret N. June 2011a, 32 pp.

Jensen K, Clausen P, Birkedal R, Kembouche Y, Christiansen E, Levin M, Koponen I, Jacobsen N, Wallin H, De Temmeman P-J et al: Standard operating procedures for characterization of the selected manufactured nanomaterials and dispersions thereof. In: Standard operating procedures for characterization of the selected manufactured nanomaterials types. Edited by Jensen K, Thieret N; 2011b.

Nordstöm, D.K. and Munoz, J.L., Geochemical Thermodynamics. Second edition. Blackwell Scientific Publications. 493 pp. (1994)

Förster H. and Tiesler H. (1993) Contribution to comparability of in vitr and in vivo man-made mineral fibre (MMMF) durability experiments. Glastechnology Bereitung 66/10, 255-266.

Osmond-McCloud, M.J., Poland C.A., Murphy F., Waddington L., Morris H., Hawkins S.C., Clark S., Aitken R., McCall M.J., Donaldson K. (2011) Durability and inflammogenic impact of carbon nanotubes compared with asbestos fibres. Particles and Fibre Toxicology 8:15.

Sebastian K., Fellman J., Potter R., Bauer J., Searl A., de Meringo A., Maquin B., de Reydellet A., Jubb G., Moore M., Preininger R., Zoitos B., Boymel P., Steenberg T., Madsen AL., Guldberg M. (2002) EURIMA test guideline: In vitro acellular dissolution of man-made vitrous silicate fibres. Glass Science Technology 75/5, 263-270.

Wiecinski, P.N., Metz K.M., Mangham, A.N., Jacobson, K.H., Hamers, R.J., Pedersen, J.A (2009) Gastrointestinal biodurability of engineered nanoparticles: Development of an in vitro assay NANOTOXICOLOGY Volume: 3   Issue: 3   Pages: 202-U66

Xia T., Kovochich M., Brant J., Hotze M., Sempf J., Oberley T., Sioutas C., Yeh J.I., Wiesner M.R., Nel, A.E. (2006) Comparison of the abilities of ambient and manufactured nanoparticles to induce cellular toxicity according to an oxidative stress paradigm, Nano Letters 6/8, 1794-1807.

Xinyuan L., Robert H.H. Agnes K.B. (2010) Biodurability of single-walled carbon nanotubes depends on surface functionalization. CARBON 48/7, 1961-1969

57

Appendix A: Protocol for Sensor Dish Reader (SDR) analyses of MN hydrochemical reactivity and biodurability.

Chemicals and Equipment
- Gamble's solution = GS. (see Table B.1)
- Revco RCO3000T-9-VBC Cell Incubator (5% CO2; 37C)
- Vortex system (IKA VIBRAMIX-VXR)
- Sensor Dish Reader 305 and 315 (PreSens Precision Sensing GmbH, Germany)
- 1 Oxydish® OD24 for O_2 measurements (PreSens Precision Sensing GmbH, Germany)
- 1 Hydrodish® HD24 for pH measurements (PreSens Precision Sensing GmbH, Germany)
- Software: SDR_v38.exe (methods and data-logging)
- Computer for the SDR_v38.exe software
- 20,000 RCF Centrifuge (Ole Dich)

The specific equipments listed above are not mandatory, but similar equipment is required
For all preperations, verified elementally clean Nanopure water is used as the source of water. Elemental water analysis is needed to ensure purity of water.
Specifications of Nanopure Diamond UV water:
Purification system is designed to 4 stages of de-ionization combined with UV light-treatment:
Resistivity: $\leq$ 18.2 MΩ-cm at 25ºC
Pyrogens: < 0.001 EU/ml
Total Organic Carbon: < 3.0 ppb
Other: nuclease-free (RNase andDNase).
Filter: 0.2 μm filter (γ-irradiated Barnstead D3750 Hollow fibre filter)

Solubility and hydrochemical reactivity screening using the SDR system
The SDR system can only be used for monitoring the pH reactivity and O_2 variation in NPs dispersions with a pH range between 5 and 9. Real-time monitoring is done using the SDR incubation dishes mounted with sensors for online pH and O_2 concentration measurements. Relevant test conditions are maintained by placing the whole system in a cell incubation oven with a well-controlled atmosphere (37°C and 5% CO_2 air supply).

Protocol
The mesurements are made in order to measure the chemical reactivity of the particles in hydrous media (e.g., NM dispersion media, synthetic lung lining fluid, and cell media). The end points are pH and oxygen concentration (O_2). The tests are run as duplicate exposures in three doses (0.08, 0.16 and 0.32 mg/ml) for each substance. The experiments run 24 hours in 24-well trays with internal sensors.
1) Dispense proportionate volumes of media (GS)$^£$ in SDR pH (white sensor) and O2 (orange-red sensor) plates
- Use well A1 for the highest dose 0.32mg/ml
- Level A: 1.872 mL; series B: 1.936 ml; range C: 1.968 and series D: 2 ml media(GS)
- The last well is always 2 ml of pure media control

2) Place the SDR plates on the respective readers (carefully ensure that the SDR plates are placed on the correct readers). Check that they are in the right position and make three point measurements

using the program "single measurement" command. - This is done to confirm that the sensors are working and also establish a general 0-reference.
- Press 3 times the "single measurement" with Tab enabled reader 305
- Press 3 times on "single measurement" with Tab enabled reader 315).

3) Dispense the appropriate doses into the wells of pH and O_2 plates
- Start with the highest dose of the first test material in well A1
- Row 1: 0.128 mL; Row 2: 0.064 mL; range 3: 0.032 ml.

4) Place the pH and O_2 SDR plates on SDS read and check that they are in the right position

5) Start measurement by pressing the "Start Measurement"

6) After 1 hour the sample rate changed to 15 min
Set a measurement on pause by pressing "Start / Stop"
- Change the sample rate to 15 min
- Accept that this change sættings for all readers - click "yes"
  Start the measurement again

7) After a total of 24 hours, end the measurement.
- stop data recording
- stop the vortes shaker
- taken the SDR plates out for sampling of the liquids filtration and centrifugation

£ Gamble's solution adjusted to pH 7.4 .

Filtration and centrifugation:
The samples are filtered and centrifuged for subsequent chemical analysis .
1) The sample for the highest dose and the reference medium is sampled by syringe and filtered through a 0.2μm CAMECA filter syringe. To obtain a dublicate, the high-dose sample from both the pH and O_2 is sampled (allows 4 mL for each material in duplicate).
- The sample is taken by inserting the tip of the syringe down to the bottom of the well and then the liquid is pumped in and out until the sample is well suspended.
- Then all the liquid is sampled (there may be a little trace of liquid left in the edge of the well, which cannot be sampled)

2) Filter the sample through a 0.2μm CAMECA filter and lead the filtrate into an acid-washed collected tube. This should produce almost 3.5 ml of liquid per sample.
3) Sample 2 x 1.5 ml of each filtered sample by pipette and enter it into 2 ml acid-washed Eppendorf tubes.
4) Centrifuge the filtered samples in the Eppendorf tubes for 60 minutes at 20,000 G using an Ole Dich centrifuge set to slow de-acceleration and 25°C.
- Place the particle samples in the outer ring, which is yield highest RCF.
- Place the media controls in the inner ring, which yield lower RCF.

5) After centrifugation, sample the upper 1.25 ml of the fluid from each pair of the centrifuge tube by pipette, and pool these into a 5-10 ml acid washed centrifuge tube. This solution is used for chemical

analysis. The pipetted volume is added an additional 1 ml of 2% ultra-pure HNO_3 in nano-pure water to prevent reprecipitation.
6) The liquid samples are stored in darkness at room temperature until analysed.

Test media used for this report:
Three media were used for the 24-hour reactivity and dissolution studies in this report. These comprised 0.05% BSA as defined in the generic NANOGENOTOX dispersion report (Jensen et al., 2011a), the EURIMA low-Ca Gambles solution tabulated below (Table A.1), and Caco 2 cell medium.

The Gamble's solution (Table A.1) is the low-Ca solution given by Sebastian et al. (2005). The chemicals are dissolved in 2 L Nanopure water (Nanopure Diamond UV) and placed in an ultrasonic bath for 15 min. Thereafter, the solution is filtered through a 0.45μm sterile filter. The final solution is added 6ml of 4 % formaldehyde per 2 L Gamble´s solution to avoid growth and placed in darkness in the refrigerator.

Table A.1: *Composition of the EURIMA low-Ca Gamble´s solution*

Compounds	Concentration [mg/ml]
NaCl	6600
$NaHCO_3$	2703
$CaCl_2$	22
$Na_2HPO_4.12H_2O$	358
Na_2SO_4	79
$MgCl.6H_2O$	212
$H_2NCH_2CO_2H$ (glycerine)	118
Na_2-citrate.$2H_2O$	153
Na_3-citrate.$2H_2O$	180
Na-pyrovate	172
Na-Lactate	175
HCl (1:1)[€]	1.1 – 1.5

[€]Used to adjust pH to 7.4 prior to testing

● Contact ●

Website:
www.nanogenotox.eu
E-mail:
nanogenotox@anses.fr

Coordinator: French Agency for Food, Environmental and Occupational Health & Safety (ANSES)
27-31, avenue du Général Leclerc
94701 Maisons-Alfort Cedex
France

Partners

French Agency for Food, Environmental and Occupational Health Safety (France)	ANSES	anses
Federal Institute of Risk Assessment (Germany)	BfR	BfR
French Atomic Energy Commission (France)	CEA	cea
Institute of Mineralogy and Crystallography (Bulgaria)	IMC-BAS	
Veterinary and Agrochemical Research Centre (Belgium)	CODA-CERVA	
Finnish Institute of Occupational Health (Finland)	FIOH	Finnish Institute of Occupational Health
Roumen Tsanev Institute of Molecular Biology Academy of Sciences (Bulgaria)	IMB-BAS	
Institut national de recherche et de sécurité (France)	INRS	inrs
National Health Institute Doutor Ricardo Jorge (Portugal)	INSA	
Scientific Institute of Public Health (Belgium)	IPH	isp WIV
Institut Pasteur of Lille (France)	IPL	Institut Pasteur de Lille
Istituto superiore di sanità (Italy)	ISS	
The Nofer institute of Occupational Medicine (Poland)	NIOM	
National Research Centre for the Working Environment (Denmark)	NRCWE	NATIONAL RESEARCH CENTRE FOR THE WORKING ENVIRONMENT
National Institute for Public Health and the Environment (The Netherlands)	RIVM	rivm
Universitat Autònoma de Barcelona (Spain)	UAB	UAB Universitat Autònoma de Barcelona

anses
French agency for food, environmental
and occupational health & safety

NANOGENOTOX

Co-funded by
the Health Programme
of the European Union

Grant Agreement n° 2009 21 01